

UNCLASSIFIED

AD NUMBER
ADB072085
NEW LIMITATION CHANGE
TO Approved for public release, distribution unlimited
FROM Distribution authorized to U.S. Gov't. agencies only; Test and Evaluation; JAN 1983. Other requests shall be referred to Air Force Rocket Propulsion Laboratory, ATTN: STINFO/TSPR, Edwards AFB, CA 93523.
AUTHORITY
AFRPL ltr dtd 6 Dec 1985

THIS PAGE IS UNCLASSIFIED

AD B072085

AUTHORITY:

AFRPL 1tr 6 Dec 85





AFRPL TR-82-038

AD:

Final Report
for the period
October 1978 to
May 1982

Retrieval of Flow-Field Temperature and Concentration of Low- Visibility Propellant Rocket Exhaust Plumes

January 1983

Author:
S. J. Young

Aerospace Corporation
El Segundo, CA 90245

TR-0082(2623)-2

Subject: Rocket Exhaust Plumes

This document contains information for manufacturing or using munitions of war. Exporting this information or releasing it to foreign nationals living in the United States without first obtaining an export license violates the International Traffic in Arms Regulations. Under 22 USC 2776, such a violation is punishable by up to 2 years in prison and by a fine of \$100,000.

Distribution limited to U.S. Government agencies only; Test and Evaluation, January 1983. Other requests for this document must be referred to AFRPL/ST-4 (Store 24), Edwards AFB, CA 93523.

DTIC FILE COPY

32728

prepared for the:

**Air Force
Rocket Propulsion
Laboratory**

Air Force Space Technology Center
Space Division, Air Force Systems Command
Edwards Air Force Base,
California 93523

DTIC
ELECTIC
MAR 31 1983

88 03 31 00 7

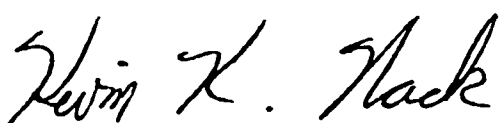
NOTICES

When U.S. Government drawings, specifications, or other data are used for any purpose other than a definitely related Government procurement operation, the Government thereby incurs no responsibility nor any obligation whatsoever, and the fact that the Government may have formulated, furnished, or in any way supplied the said drawings, specifications, or other data is not to be regarded by implication or otherwise, or in any manner licensing the holder or any other person or corporation, or conveying any rights or permission to manufacture, use of sell any patented invention that may in any way be related hereto.

FOREWORD


This final report was submitted by the Aerospace Corporation, El Segundo, California 90245, under Contract No. F04701-81-C-0082 with the Air Force Rocket Propulsion Laboratory, Edwards AFB, California 93523, under Air Force Project Task 573010CU. The report documents the development of the Emission/Absorption Inversion Code (EMABIC). A User's Manual which describes the operation of the EMABIC code has also been published as AFRPL-TR-82-37.

This report has been reviewed and is approved for publication in accordance with the distribution statement on the cover and on the DD Form 1473.


KEVIN K. NACK, 1Lt, USAF
Project Manager


WILBUR C. ANDREPONT
Chief, Plume Technology Branch

FOR THE DIRECTOR


JOHN C. KOGER, Lt Col, USAF
Chief, Propulsion Analysis Division

REPORT DOCUMENTATION PAGE		READ INSTRUCTIONS BEFORE COMPLETING FORM	
1. REPORT NUMBER AFRPL-TR-82-038	2. GOVT ACCESSION NO. AD-13072	3. RECIPIENT'S CATALOG NUMBER 885	
4. TITLE (and Subtitle) RETRIEVAL OF FLOW-FIELD TEMPERATURE AND CONCENTRATION OF LOW-VISIBILITY PROPELLANT ROCKET EXHAUST PLUMES		5. TYPE OF REPORT & PERIOD COVERED Final Report Oct 78 - May 82	
		6. PERFORMING ORG. REPORT NUMBER TR-0082(2623)-2	
7. AUTHOR(s) Stephen J. Young		8. CONTRACT OR GRANT NUMBER(s) F04701-81-C-0082	
9. PERFORMING ORGANIZATION NAME AND ADDRESS The Aerospace Corporation El Segundo, Calif. 90245		10. PROGRAM ELEMENT, PROJECT, TASK AREA & WORK UNIT NUMBERS 573010CU	
11. CONTROLLING OFFICE NAME AND ADDRESS Air Force Rocket Propulsion Laboratory/DYP Edwards Air Force Base, Calif. 93523		12. REPORT DATE January 1983	
		13. NUMBER OF PAGES 64	
14. MONITORING AGENCY NAME & ADDRESS (if different from Controlling Office) Space Division Air Force Systems Command Los Angeles, Calif. 90009		15. SECURITY CLASS. (of this report) UNCLASSIFIED	
		15a. DECLASSIFICATION/DOWNGRADING SCHEDULE	
16. DISTRIBUTION STATEMENT (of this Report) Distribution limited to U.S. Government Agencies; Test Evaluation: November JAN 1983 1982 . Other request for this document must be referred to AFRPL (STINFO/TSPR), Edwards CA 93523.			
17. DISTRIBUTION STATEMENT (of the abstract entered in Block 20, if different from Report)			
18. SUPPLEMENTARY NOTES			
19. KEY WORDS (Continue on reverse side if necessary and identify by block number) Emission and Absorption Inversion Low-Visibility Rocket Plumes Plume Diagnostics Retrieval Diagnostics Rocket Plume Emission			
20. ABSTRACT (Continue on reverse side if necessary and identify by block number) Diagnostic procedures based on iterative Abel inversion have been developed and tested for retrieving both the particle- and gas-phase properties of low-visibility propellant rocket exhaust plumes. The required input data consist of transverse scans of the plume infrared radiance and transmittance at wavelengths in and just outside the gas emission band; data also include transverse scans of angular laser scattering efficiency at the off-band wavelength. From these data, retrieval can be made for the particle volume scattering and volume absorption cross sections, scattering phase function,			

UNCLASSIFIED

SECURITY CLASSIFICATION OF THIS PAGE(When Data Entered)

19. KEY WORDS (Continued)

20. ABSTRACT (Continued)

) particle temperature, gas temperature, and gas concentration. The diagnostics are limited to particle loading levels small enough to justify the use of the single-scattering approximation.

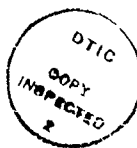
Example applications are made to three plume models containing $\text{Al}_2\text{O}_3/\text{H}_2\text{O}$, C/HCl , and $\text{ZrO}_2/\text{H}_2\text{O}$ as the particle and gas phases. For all cases, accurate and unique retrieval of the flow-field properties from exact "synthesized" transverse data is demonstrated.

UNCLASSIFIED

SECURITY CLASSIFICATION OF THIS PAGE(When Data Entered)

CONTENTS

1.	INTRODUCTION.....	7
1.1	Background.....	7
1.2	Scope of Present Study.....	11
1.3	Emission/Attenuation/Scattering Data Requirements.....	12
2.	RADIATION TRANSPORT EQUATIONS.....	15
2.1	General Line-of-Sight Equations.....	15
2.2	Transformation to Cylindrical Coordinates.....	20
2.3	Laser Scattering Equation.....	23
3.	RETRIEVAL PROCEDURES.....	25
3.1	Introduction.....	25
3.2	Retrieval of $\gamma(r)$	28
3.3	Retrieval of $\alpha(r)$, $\beta(r)$, and $p(r, \theta)$	30
3.4	Retrieval of $T_p(r)$	31
3.5	Retrieval of $T_g(r)$ and $\bar{\kappa}(r)$	32
4.	APPLICATION.....	33
4.1	Plume Model Summary.....	33
4.2	Emission/Attenuation Profiles and Laser Scattering Results.....	41
4.3	Particle Retrieval Results.....	54
4.4	Gas Retrieval Results.....	56
5.	SUMMARY AND CONCLUSIONS.....	63



Accession For	
NTIS GRA&I	<input type="checkbox"/>
DTIC TAB	<input checked="" type="checkbox"/>
Unannounced	<input type="checkbox"/>
Justification	
By	
Distribution/	
Availability Codes	
Dist	Avail and/or Special
B	

FIGURES

1. Data Measurement Geometry.....	14
2. General Scattering Geometry.....	16
3. Cylindrical Plume Scattering Geometry.....	21
4. Iterative Abel Inversion Algorithm.....	26
5. Radial Temperature Profiles for the MSP Plume Model.....	35
6. Radial Temperature Profiles for the ALP Plume Model.....	36
7. Radial Profiles for the RSP Plume Model.....	37
8. Differential Scattering Cross Section for Al_2O_3	38
9. Differential Scattering Cross Section for C.....	39
10. Differential Scattering Cross Section for ZrO_2	40
11. Transverse Radiance Profiles for the MSP Plume Model.....	42
12. Transverse Extinctance Profiles for the MSP Plume Model.....	43
13. Transverse Radiance Profiles for the ALP Plume Model.....	44
14. Transverse Extinctance Profiles for the ALP Plume Model.....	45
15. Transverse Radiance Profiles for the RSP Plume Model.....	46
16. Transverse Extinctance Profiles for the RSP Plume Model.....	47
17. Angle Variation of Scattering Efficiency Function for the MSP Plume Model.....	48
18. Transverse Variation of Scattering Efficiency Function for the MSP Plume Model.....	49
19. Angle Variation of Scattering Efficiency Function for the ALP Plume Model.....	50
20. Transverse Variation of Scattering Efficiency Function for the ALP Plume Model.....	51
21. Angle Variation of Scattering Efficiency Function for the RSP Plume Model.....	52

FIGURES (Continued)

22. Transverse Variation of Scattering Efficiency Function for the RSP Plume Model.....	53
23. Particle Properties Retrieval Errors for the RSP Plume Model.....	55
24. Gas Temperature Retrieval Results for the MSP Plume Model.....	57
25. Gas Concentration Retrieval Results for the MSP Plume Model.....	58
26. Gas Temperature Retrieval Results for the ALP Plume Model.....	59
27. Gas Concentration Retrieval Results for the ALP Plume Model.....	60
28. Gas Temperature Retrieval Results for the RSP Plume Model.....	61
29. Gas Concentration Retrieval Results for the RSP Plume Model.....	62

TABLES

1. E/A Transfer Equations in Cylindrical Coordinates and in Source Function-Kernel Product Form.....	29
2. Summary of Plume Model Data.....	34

1. INTRODUCTION

1.1 Background

For the past few years, the Air Force Rocket Propulsion Laboratory (AFRPL) has sponsored a series of theoretical and experimental programs on the retrieval of plume flow-field properties by analysis of the infrared radiative and absorptive properties of plumes. This report continues the third phase of study in these programs by The Aerospace Corporation. The first phase (Ref. 1) was a study of the classic problem of retrieving radial profiles of gas temperature and concentration in cylindrically-symmetric, gaseous plumes from transverse emission and absorption (E/A) profiles obtained in a fixed spectral bandpass. The E/A profiles are defined in terms of the radial profiles of pressure, temperature, and concentration (pTc profiles) by integral equations of radiative transfer. Retrieval of the pTc profiles from the E/A profiles involves a numerical inversion of these integral equations.

In this first phase study, an inversion procedure was developed and incorporated into the computer code EMABIC. The inversion algorithm is an iterative Abel inversion. The well-known Abel inversion procedure is valid for optically thin sources; for the general case of optical thickness, an iterative procedure is required. The code has been applied to several synthetic and experimental data and performs satisfactorily as a diagnostic for most gas-only plume problems. Some problems occur when the temperature

-
1. S. J. Young, Inversion of Plume Radiance and Absorptance Data for Temperature and Concentration, AFRPL-TR-78-60, U. S. Air Force Rocket Propulsion Laboratory, Edwards Air Force Base, California, 29 September 1978.

profile has a deep minimum on the plume axis or when the input E/A profiles are particularly noisy, even if they are adequately smoothed. This is an inherent feature of inversion, however, and is not restricted to the method of inversion. A similar inversion code has been developed at the Arnold Engineering Development Center (AEDC) (Ref. 2). Recently, a random error propagation routine was added to EMABIC so that retrieval error could be estimated automatically from E/A measurement error (Ref. 3).

The second phase of study was the consideration of multispectral inversion and the effects of particle loading in tactical motor plumes. In multispectral inversion, retrieval is made on the basis of how E/A spectra vary in wavelength for a fixed measurement line of sight. It was found that this inversion scheme is not applicable in the infrared on either a monochromatic or wide band spectral scale near the exit plane for small plumes with mild temperature gradients, such as those characteristic of tactical rocket motors. Even under ideal circumstances, temperature and concentration retrieval errors up to 30% were encountered. The failure of the method is caused by the lack of spatial resolution inherent in the inversion weighting functions. Results of this study are reported in Ref. 4. Because this method failed for purely gaseous plumes, it was never applied to two-phase plumes.

-
2. C. C. Limbaugh, W. T. Bertrand, E. L. Kiech and T. G. McRae, Nozzle Exit Plane Radiation Diagnostics Measurements of the Improved Transtage Liquid Rocket Injector Program, AEDC-TR-79-29, ARO Inc., Arnold Engineering Development Center, Arnold Air Force Station, Tennessee, March 1980.
 3. S. J. Young, Random Error Propagation Analysis in the Plume Diagnostic Code EMABIC, AFRPL-TR-81-59, U. S. Air Force Rocket Propulsion Laboratory, Edwards Air Force Base, California, July 1981.
 4. S. J. Young, Multicolor Inversion Diagnostic for Tactical Motor Plumes, AFRPL-TR-80-30, U. S. Air Force Rocket Propulsion Laboratory, Edwards Air Force Base, California, May 1980.

It was decided to revert to the multiposition inversion diagnostic of the first study phase and to pursue its application to two-phase, tactical rocket motor plumes.

The primary goal of the first part of this third phase was to determine quantitative limits of particle loading in realistic tactical rocket motor plumes for which the gas properties of the plume could be retrieved with standard E/A inversion diagnostics without having to account for the radiating, absorbing, and scattering effects of the particles. The procedure was to assume flow-field properties for two-phase plumes of interest, generate E/A profiles* with account of particles using a single-scattering plume radiation code (EAPROF, Ref. 5), retrieve the gas properties from the E/A profiles with the gas-only inversion code EMABIC under the assumption that the profiles were caused by gas alone, and compare the retrieved gas properties with the assumed properties. Generally, the degree of particle loading was treated as a parameter. The work focused on tactical rocket motors where the particle loading level is small, that is, to motors where the particulate material is added to the fuel only as a stabilizer (e.g., Al_2O_3), or to motors where the plume particulate results from chemical reactions (e.g., carbon) but not to motors in which the major fuel is itself a metal. The procedure was applied to a minimum smoke propellant (MSP) model, an advanced liquid propellant (ALP)

* When particle effects are accounted for, the A of E/A should more properly be interpreted as "attenuation" rather than just absorption since signal reduction by particle scattering is included. In this report, "extinction" and "extinctance" are sometimes used, along with "attenuation," to denote the combined effects of absorption and scattering.

5. S. J. Young, User's Manual for the Plume Signature Code EAPROF, AFRPL-TR-81-08, U. S. Air Force Rocket Propulsion Laboratory, Edwards Air Force Base, California, January 1981.

model, and a reduced smoke propellant (RSP) model. The results are reported in Ref. 6.

Two important results were obtained. The first is that the limit of particle loading at which reasonable ($< 10\%$ error) retrieval results can be obtained is generally smaller than the nominal loading level for the plume. The important implication of this result is that, to the extent that the systems studied are typical, E/A diagnostics on plumes generated by even low- and reduced-smoke type propellants require some account of particle effects. The second result is that the maximum loading level for acceptable gas temperature retrieval is much higher (about an order of magnitude) than that for gas concentration retrieval. Consequently, in applications where temperature retrieval is of primary concern, the use of gas-only E/A diagnostics may be justified even though the total retrieval results may be substantially in error.

Analysis was also made of a procedure in which first-order corrections were made to the total gas-plus-particle E/A profiles by using particle-only E/A profiles obtained outside the gas absorption band. The corrected profiles provided better estimates to the gas-only profiles needed in the gas-only inversion. The particle loading limit for valid use of this procedure is the value for which the total extinction of radiation by particles over a full diameter of the plume is about 10 percent. (Note that if this condition is met, then the condition is also met that the attenuation by scattering alone over this path is less than about 10 percent. The latter condition is

-
6. S. J. Young, Retrieval of Flow-Field Gas Temperature and Concentration of Low-Visibility Propellant Rocket Exhaust Plumes, AFRPL-TR-82-13, U. S. Air Force Rocket Propulsion Laboratory, Edwards Air Force Base, California, March 1982.

required by the single-scattering assumption used in the work.) For the two cases (MSP and RSP) where the nominal loading limit roughly satisfied this condition, the use of the procedure resulted in retrieved gas properties that were accurate to within the convergence criteria set on the inversion. For the ALP model, the nominal loading level was well above this limit, and the retrieved results were poor.

1.2 Scope of Present Study

The present work expands the work begun in Ref. 6 in two significant aspects. First, the restriction of the first-order, off-band (FOOB) correction procedure that the plume be optically thin to total extinction is relaxed. This is accomplished essentially by using the full, two-phase, single-scattering radiation model in the inversion code EMABIC as well as in the plume radiation code EAPROF. The second significant expansion is that retrieval diagnostics for particle properties are developed. The previous work on two-phase plume diagnostics assumed that all particle properties (e.g., species, index of refraction, spatial and size distribution) were known. The current work defines procedures for retrieving the volume cross sections for particle absorption, scattering, and extinction, as well as the particle scattering phase function and radial temperature profile. (Further analysis is underway, but not reported here, on the retrieval of the particle size and radial distributions from the scattering phase function and volume extinction cross section.) The plume emission/attenuation/scattering (E/A/S) data required for application of these procedures are discussed in Section 1.3.

As in the preceding work of this phase, the analyses presented here were made with synthesized E/A/S data, that is, data computed from assumed known plume properties. No application to experimental data was made. Also, since

the main emphasis of this work was on the feasibility of retrieval and not its practical application, no treatment of random or bias error propagation was made. The radiative transfer theory used to compute these synthetic data is presented in Section 2, and the inversion procedures for retrieving the plume properties from the synthesized data are presented in Section 3. The entire prediction and inversion capabilities developed in these two sections have been written as a series of computer codes and are described in a separate report (Ref. 7). Application of the inversion procedure was made to the MSP, ALP, and RSP models described in Ref. 5. Results and discussion of the applications are made in Section 4, and a summary of conclusions drawn from the results is given in Section 5.

1.3 Emission/Attenuation/Scattering Data Requirements

The diagnostic scheme developed in Section 3 requires traditional transverse E/A data at two wavelengths and angular scattering data at one of the two wavelengths (Fig. 1). λ_1 is a spectral position at which both the gas and particles of interest radiate and absorb. λ_2 is a position at which only the particles radiate and absorb. λ_2 should be as close to λ_1 possible so that it can be assumed that the particle optical properties are the same at the two wavelengths. The transverse E/A data required at these wavelengths are

$$\left. \begin{array}{l} \bar{N}(z) \\ \bar{\tau}(z) \end{array} \right\} \quad 0 < z < R \quad \lambda = \lambda_1 \text{ (gas + particles)}$$

$$\left. \begin{array}{l} N_p(z) \\ \tau_p(z) \end{array} \right\} \quad 0 < z < R \quad \lambda = \lambda_2 \text{ (particles only)}$$

7. S. J. Young, User's Manual for the Flow-Field Diagnostics Code EMABIC, AFRL-TR-82-57, U. S. Air Force Rocket Propulsion Laboratory, Edwards Air Force Base, California, February, 1983.

where z is the transverse coordinate, R is the plume radius, N is the plume radiance, and τ is the plume transmittance to external radiation. An axisymmetric, cylindrical plume is assumed.

The scattering data are required only at λ_2 . In order to get enough scattered intensity to measure accurately, the source would probably have to be a laser. This source is scanned in the transverse direction just as the E/A sources are scanned. Angular scattering data are required between $\theta = 0$ and $\theta = \pi$ where the reference is the $z = 0$ line and the plume center line. The scattering function used in this work considers scanning from $z = 0$ to $z = R$ and angular measurements on the opposite side of the plume (as indicated in Fig. 1). The field of view of the scattered radiation sensor should be wide enough to see the entire width of the plume. Also, the distance from the sensor to the plume should be much larger than R . Figure 1 indicates a single detector that scans in θ . A more probable arrangement would be an array of detectors at various θ . In any case, the required data are

$$f(z, \theta) \quad \left\{ \begin{array}{l} 0 \leq \theta \leq \pi \\ 0 \leq z \leq R \\ \lambda = \lambda_2 \end{array} \right.$$

where f is the scattered power divided by the laser power. In general, the variation in θ is needed for each transverse position. A simplified retrieval analysis is presented later (Section 3.3) in which only the variation at $z = 0$ is required.

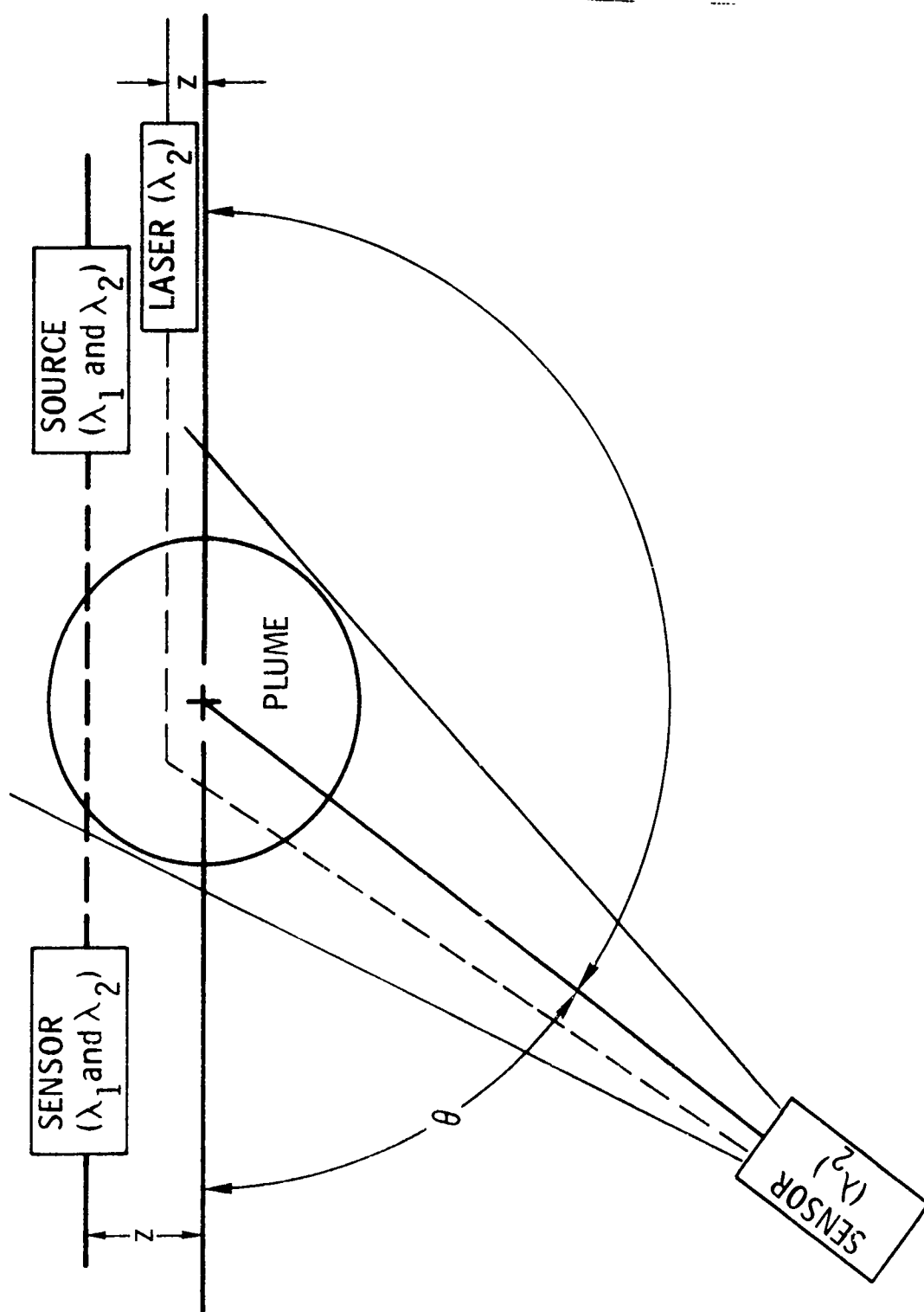


Fig. 1. Data Measurements Geometry.

2. RADIATION TRANSPORT EQUATIONS

The radiation model for predicting E/A profiles from known plume properties was derived and discussed in detail in Refs. 5 and 6. Briefly, the model treats the problem of radiative transfer in a coupled, two-phase (gas and particles) medium. Radiation transport for the gas phase is treated with the Malkmus statistical band model and the Curtis-Godson nonuniformity approximation. Radiation transport for the particle phase is treated with the single-scattering approximation. In this approximation, only radiation that is emitted directly on and along an observation line of sight, or is scattered into the line of sight by a single scattering contributes to observed emission. In transmission, no radiation scattered into the line of sight is counted as transmitted signal.

A review of this model for a line of sight through a general medium is given in Section 2.1. In Section 2.2, the equations are transformed to cylindrical coordinates for application to the plume problem, and written in a form suitable for both prediction and inversion. In Section 2.3, the addition to the model required for calculating the laser scattering function $f(z, \theta)$ is developed.

2.1 General Line-of-Sight Equations

For a line of sight s through a general two-phase medium (Fig. 2), the observed emission \bar{N} is

$$\bar{N} = \int_0^L \tau_a(s) \tau_b(s) \bar{\tau}(s) \{Q_T(s) + Q_S(s)\} ds \quad (1)$$

$$Q_T(s) = J_p(s) + y(s) J_g(s) \quad (2)$$

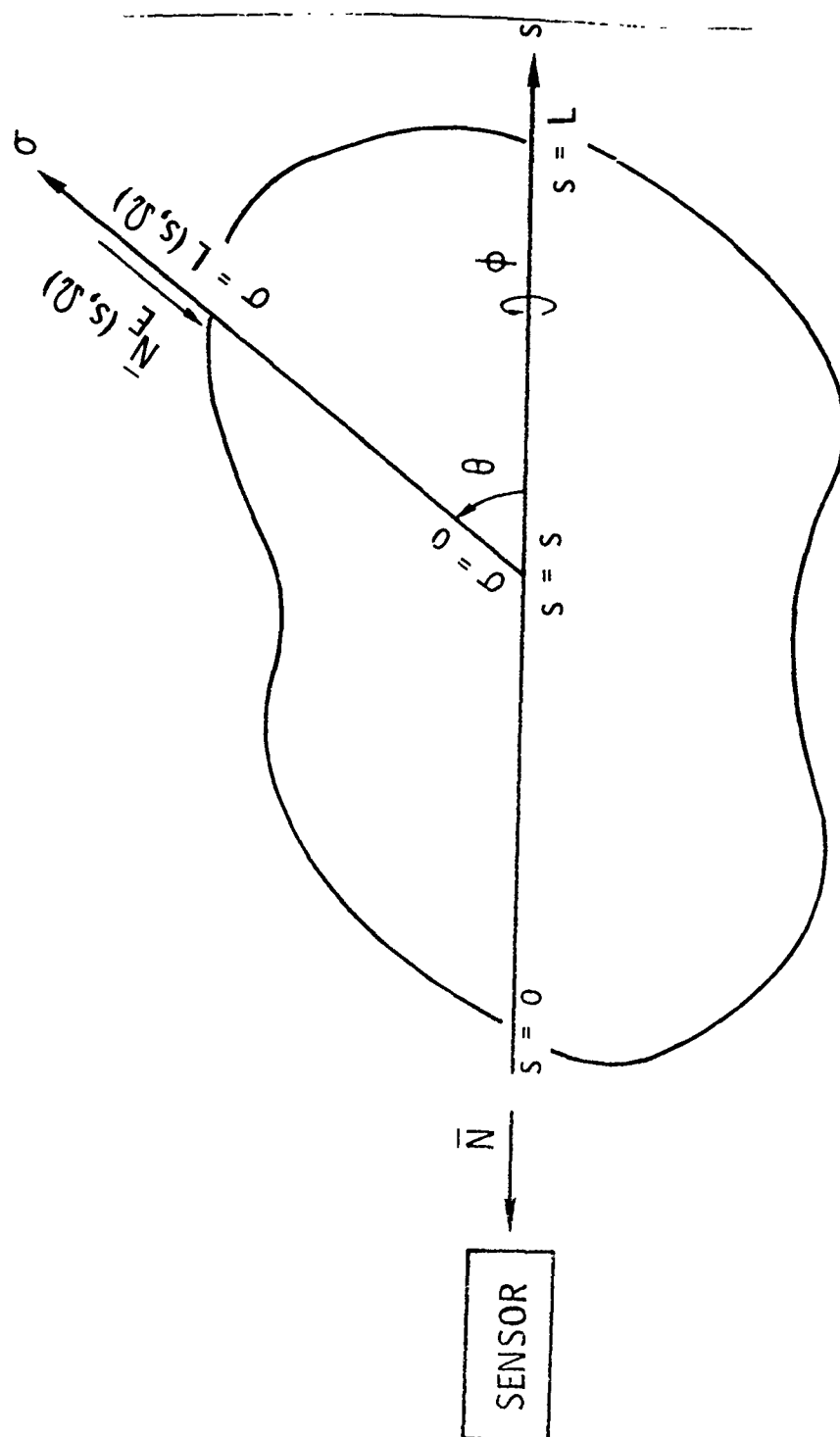


Fig. 2. General Scattering Geometry.

$$J_p(s) = \alpha(s) B_p(s) \quad (3)$$

$$J_g(s) = \bar{\kappa}(s) B_g(s) \quad (4)$$

$$Q_S(s) = \int_{4\pi} J_S(s, \Omega) [Q_E(s, \Omega) + Q_T(s, \Omega)] d\Omega \quad (5)$$

$$J_S(s, \Omega) = \frac{\beta(s)}{4\pi} p(s, \Omega) \quad (6)$$

$$Q_E(s, \Omega) = \tau_\alpha [L(s, \Omega)] \frac{\bar{\tau} [s + L(s, \Omega)]}{\bar{\tau}(s)} N_E(s, \Omega) \quad (7)$$

$$Q_T(s, \Omega) = \int_0^{L(s, \Omega)} \tau_\alpha(\sigma) \frac{\bar{\tau}(s + \sigma)}{\bar{\tau}(s)} Q_T(\sigma, s) d\sigma \quad (8)$$

$$Q_T(\sigma, s) = J_p(\sigma) + y(s + \sigma) J_g(\sigma) \quad (9)$$

$$J_p(\sigma) = \alpha(\sigma) B_p(\sigma) \quad (10)$$

$$J_g(\sigma) = \bar{\kappa}(\sigma) B_g(\sigma). \quad (11)$$

All of the quantities appearing in these equations have been defined in Ref. 6, and only a brief explanation will be given here. $\tau_\alpha(\sigma)$ is the transmittance between $s = 0$ and general position s effected by particle absorption. $\tau_\beta(s)$ and $\bar{\tau}(s)$ are the corresponding transmittances for particle scattering and gas absorption. Q_T is the thermal source function and is composed of the particle component $J_p(s)$ and the gas component $J_g(s)$. $\alpha(s)$ and $\beta(s)$ are the

volume cross sections* for particle absorption and scattering, respectively, and $\bar{\kappa}(s)$ is the volume cross section for gas absorption. $y(s)$ is a band model function that accounts for the deviation of band absorption from the Lambert and Beer absorption laws, and varies with assumed spectral lineshape and approximation used to treat the optical path nonuniformity. $B_p(s)$ and $B_g(s)$ are the Planck function evaluated at the particle and gas temperatures at s , respectively. Q_S is the scattering source function and is an integral over all directions of radiation arriving at s from the scattering line of sight σ . Ω is the scattering solid angle described by the scattering angle θ and azimuthal angle ϕ . The integration weight given to each scattering line of sight is $J_S(s, \Omega)$ and is directly proportional to the particle scattering phase function $p(s, \Omega)$. Q_E is the contribution to Q_S from external radiation $N_E(s, \Omega)$ incident at the boundary position $\sigma = L(s, \Omega)$. τ_α and $\bar{\tau}$ are particle and gas transmittances, respectively, for the indicated path lengths. $Q_T(s, \Omega)$ is the thermal contribution to Q_S from the scattering line of sight. All of the quantities comprising Q_T are as previously explained, except that they are written for the line-of-sight variable σ rather than s .

The transmission through the medium along the observation line of sight s is given by

$$-\ln \bar{\tau} = \int_0^L [\gamma(s) + \bar{\kappa}(s) y(s)] ds \quad (12)$$

$$\gamma(s) = \alpha(s) + \beta(s) \quad (13)$$

*"Volume cross section" is a cross section per unit volume of scattering or absorbing centers and has the unit of inverse length. For example, $\alpha(s) = n_p(s) \sigma_a(s)$ where n_p is particle number density and σ_a is the Mie absorption cross section. In Ref. 6, these quantities were referred to as "coefficients."

where $\gamma(s)$ is the volume extinction cross section.

Equations (1) and (2) are used to compute the combined gas-plus-particle E/A profiles at λ_1 . The particle-only equations that are appropriate for the off-band spectral position λ_2 are obtained by setting $\bar{\kappa} = 0$ ($y \equiv \bar{\tau} \equiv 1$). The results for particle-only radiance and transmittance are

$$N_p = \int_0^L \tau_\alpha(s) \tau_\beta(s) \{Q_T(s) + Q_S(s)\} ds \quad (14)$$

$$Q_T = J_p(s) \quad (15)$$

$$J_p(s) = \alpha(s) B_p(s) \quad (16)$$

$$Q_S(s) = \int_{4\pi} J_S(s, \Omega) [Q_E(s, \Omega) + Q_T(s, \Omega)] d\Omega \quad (17)$$

$$J_S(s, \Omega) = \frac{\beta(s)}{4\pi} p(s, \Omega) \quad (18)$$

$$Q_E(s, \Omega) = \tau_\alpha [L(s, \Omega)] N_E(s, \Omega) \quad (19)$$

$$Q_T(s, \Omega) = \int_0^L \tau_\alpha(\sigma) Q_T(\sigma, s) d\sigma \quad (20)$$

$$Q_T(\sigma, s) = J_p(\sigma) \quad (21)$$

$$J_p(\sigma) = \alpha(\sigma) B_p(\sigma) \quad (22)$$

and

$$-\ln \tau_p = \int_0^L \gamma(s) ds. \quad (23)$$

The gas-only equations are obtained by setting $\alpha = \beta = p = 0$ ($\tau_\alpha \equiv \tau_\beta \equiv 1$). The gas-only radiance and transmittance are

$$\bar{N}_g = \int_0^L \bar{\tau}(s) Q_T(s) ds \quad (24)$$

$$Q_T(s) = y(s) J_g(s) \quad (25)$$

$$J_g(s) = \bar{\kappa}(s) B_g(s) \quad (26)$$

and

$$-\ln \bar{\tau}_g = \int_0^L \bar{\kappa}(s) y(s) ds. \quad (27)$$

2.2 Transformation to Cylindrical Coordinates

Thus far, the radiation formulation has been developed in terms of the observation line-of-sight variable s . For the cylindrical geometry of an axisymmetric plume, the radial coordinate r is a more natural coordinate. The mathematical detail of carrying out the transformation from s to r is reported in Ref. 6, and the geometry for the transformation is shown in Fig. 3. In effect, equations of the form

$$F = \int_0^L J(s) G(s) ds, \quad (28)$$

where the integration is over the full extent of a chord located a transverse distance z from the cylinder diameter, and $J(s)$ is a function only of radius, are transformed into

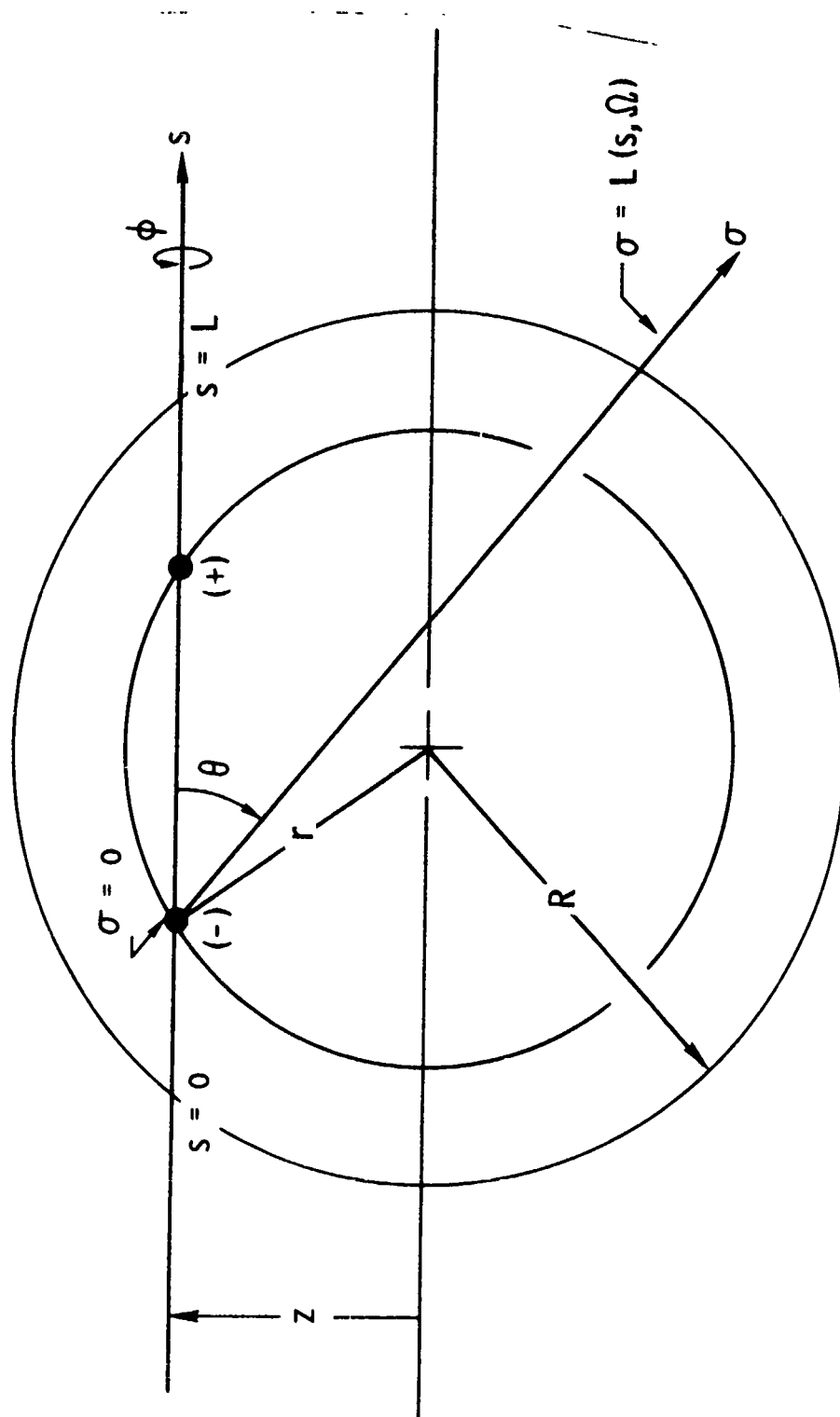


Fig. 3. Cylindrical Plume Scattering Geometry.

$$F(z) = 2 \int_z^R J(r) G(z,r) \frac{rdr}{(r^2 - z^2)^{1/2}} \quad (29)$$

where R is the cylinder radius, and

$$G(z,r) = \frac{1}{2} [G^+(z,r) + G^-(z,r)]. \quad (30)$$

$G^+(z,r)$ and $G^-(z,r)$ are the values of G at the two intersections (Fig. 3) of the chord s at z with the circle of radius r . The reason for the transformation to the form of Eq. (29) is not that it facilitates the calculation of E/A profiles (computer coding for the coordinate s is, in fact, somewhat easier and more straightforward than for r , and was employed in the previous code EAPROF), but that this form is required by the inversion procedure used in this work (Section 3) to obtain the source function $J(r)$ from a given $F(z)$. For predicting E/A profiles from known plume properties, the kernel $G(z,r)$ is a known function. In inversion, it is iteratively computed from the retrieved plume properties of the previous iteration.

The transformations of the observation line-of-sight equations [(i.e., Eqs. (1), (12), (14), (23), (24), and (27)] to the form of Eq. (29) are summarized in Table 1. The factoring of the integrands of these equations into the product from $J(r) G(z,r)$ was based on the fact that only the variables α , β , $p(\Omega)$, $\bar{\kappa}$, B_g , and B_p (and thus also J_g and J_p) are functions of r alone, and was performed to isolate the particle source functions in the particle-only equations and the gas source functions in the gas-only and the coupled gas-plus-particle equations. The factoring for the particle-only and coupled gas-plus-particle equations also makes the kernel function an explicit function of the source function J . In E/A profile prediction, this explicit dependence of G on J is of inconsequential concern, and in inversion it is handled by using the previous iteration result for J in calculation G .

The actual procedures for computing the various components of G have been discussed previously: $\tau^{\pm}(z,r)$ and $y^{\pm}(z,r)$ in Ref. 1 and $Q_S^{\pm}(z,r)$ in Ref. 6. The particle transmittances $\tau_{\alpha}^{\pm}(z,r)$ and $\tau_{\beta}^{\pm}(z,r)$ are computed in the same manner as the gas transmittances $\tau^{\pm}(z,r)$.

2.3 Laser Scattering Equation

The scattered radiance at angle θ from a beam traversing the chord s for the case where only single-scattering is important is*

$$I(\theta) = \frac{I_0}{4\pi} \frac{A}{D^2} \int_0^L \beta(s) p(s,\theta) \exp \left[-\int_0^s \gamma(s') ds' - \int_0^{L(s,\theta)} \gamma(\sigma) d\sigma \right] ds \quad (37)$$

where I_0 is the incident beam flux, A is the sensor entrance aperture area, D is the distance from the plume axis to the sensor (it is assumed that $D \gg R$), p is the scattering phase function, and σ is the scattering path coordinate. The integration over s indicates that the detector field of view encompasses the entire plume diameter. The exponential factor accounts for extinction along the path from $s = 0$ to $s = s(\sigma = 0)$ and then on to $\sigma = L(s,\theta)$. With the definitions

$$J(s,\theta) = \frac{\beta(s)}{4\pi} p(s,\theta), \quad (38)$$

$$g(s,\theta) = \exp \left\{ -\int_0^s \gamma(s') ds' - \int_0^{L(s,\theta)} \gamma(\sigma) d\sigma \right\} \quad (39)$$

* The geometry of Fig. 3 is applicable to the laser scattering problem by interpreting s as the incident axis for radiation, σ as the exit scattering line of sight, and considering scattering only within the plane of the figure ($\phi = \pi/2$).

and

$$f(\theta) = \frac{I(\theta)}{I_0} \frac{D^2}{A}, \quad (40)$$

Eq. (37) can be written as

$$\tilde{f}(\theta) = \int_0^L J(s, \theta) g(s, \theta) ds. \quad (41)$$

As for the E/A equations, this result is now transformed to cylindrical coordinates. The result is

$$f(z, \theta) = 2 \int_z^R J(r, \theta) G(z, r, \theta) \frac{r dr}{(r^2 - z^2)^{1/2}} \quad (42)$$

where

$$J(r, \theta) = \frac{\beta(r)}{4\pi} p(r, \theta), \quad (43)$$

$$G(z, r, \theta) = \frac{1}{2} [g^+(z, r, \theta) + g^-(z, r, \theta)], \quad (44)$$

and $g^\pm(z, r, \theta)$ are the transmission functions that correspond to the two scattering paths from $s = 0$ to the far and near intersections of s with r and then on to the boundary at angle θ . The method of calculation of $g^\pm(z, r, \theta)$ is a straightforward numerical integration along the two legs of the scattering path with interpolation for γ at each point from the radial profile $\gamma(r)$.

3. RETRIEVAL PROCEDURES

3.1 Introduction

In this section, the methods for retrieving the plume flow-field properties from measured (or simulated) E/A and laser scattering data are considered. The basic method of retrieval is the application of the simple Abel and the iterative Abel inversion procedures derived in Ref. 1 to a specific transverse data profile to retrieve a specific radial profile. The procedure is described in detail in Ref. 1 and outlined here for convenience.

In general, we have an equation of the form

$$F(z) = 2 \int_z^R J(r) G[z, r, J(r)] \frac{r dr}{(r^2 - z^2)^{1/2}} \quad (45)$$

where $F(z)$ is a known transverse profile of some quantity and $J(r)$ is the desired result. The kernel function G is a known, calculable function. Its dependence on the unknown function $J(r)$ is handled by iteration in that G is calculated from the $J(r)$ of the preceding iteration. The method of solution is outlined in Fig. 4 as a calculation flow diagram. The function $F(z)$ is entered and an immediate Abel inversion is made to get a first guess for $J(r)$. This first guess would be the desired solution if $G \equiv 1$ and is

$$J(r) = - \frac{1}{2\pi r} \frac{dH(r)}{dr} \quad (46)$$

where

$$H(r) = 2 \int_r^R F(z) \frac{z dz}{(z^2 - r^2)^{1/2}} \quad (47)$$

A = ABEL INVERSION
P = F(z) CALCULATION

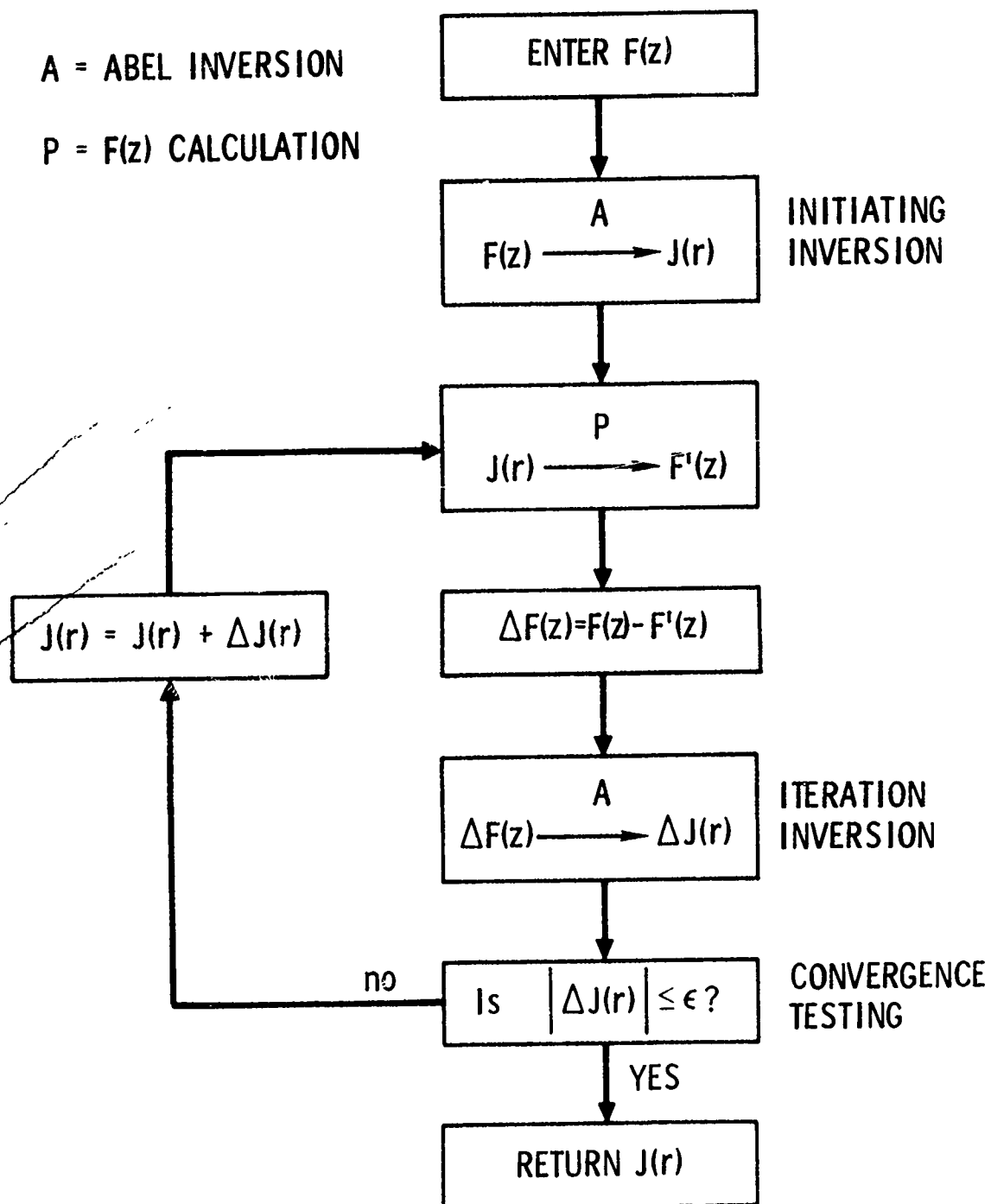


Fig. 4. Iterative Abel Inversion Algorithm.

With this first guess, a new transverse profile $F'(z)$ is calculated and subtracted from the true profile. An Abel inversion is then made on the difference profile to obtain a correction term to $J(r)$. If the correction term is less than some convergence criterion ϵ , the inversion is complete. Otherwise, the correction is made to $J(r)$ and the process is repeated by calculating a new transverse profile $F'(z)$ with the new $J(r)$.

The input transverse profiles required by the inversion procedure are (as described in Section 1.3) as follows:

- $\bar{N}(z)$ coupled gas/particle radiance at λ_1
- $\bar{T}(z)$ coupled gas/particle transmittance at λ_1
- $N_p(z)$ particle-only radiance at λ_2
- $T_p(z)$ particle-only transmittance at λ_2
- $f(z, \theta)$ scattering efficiency at λ_2

The first step in analysis is an Abel inversion of the particle-only transmittance profile $T_p(z)$ to get the radial profile of the volume extinction cross section $\gamma(r)$. Next, an iterative Abel inversion is made of $f(z, \theta)$ for each θ . The radial source function obtained from the inversion is $J(r, \theta) = \beta(r)p(r, \theta)/4\pi$ where $\beta(r)$ is the volume scattering cross section, and $p(r, \theta)$ is the scattering phase function. An integration of $J(r, \theta)$, over 4π steradians for each r gives $\beta(r)$. The phase function is then obtained from $p(r, \theta) = 4\pi J(r, \theta)/\beta(r)$, and the volume absorption cross section $\alpha(r) = \gamma(r) - \beta(r)$.

At this point, the optical properties of the particles (except for their temperature) are completely determined in so far as they are needed for radiation calculations. Note also that nothing has been assumed about the particles except that if they are irregularly shaped, they are randomly oriented. If assumptions are now made about what the particles are made of, what their

index of refraction is, and that they are spherical, the results [that is $\alpha(r)$, $\beta(r)$ and $p(r,\theta)$] could be further analyzed to yield the spatial and size distributions of the particles. This problem is not considered here.

The next step in the analysis is an iterative Abel inversion of the particle-only radiance $N_p(z)$ for the particle temperature $T_p(r)$. Now, all of the particle characteristics are determined, and the final step can be performed (with iterative Abel inversion) by solving the coupled gas/particle E/A profiles $\bar{N}(z)$ and $\bar{\tau}(z)$ for the gas temperature and concentration profiles.

The order in which these steps are performed is important since each step requires the results obtained in the preceding steps. The end results of the inversions are:

$T_g(r)$	Gas temperature
$c_g(r)$	Gas concentration
$T_p(r)$	Particle temperature
$\alpha(r)$	Particle volume absorption cross section
$\beta(r)$	Particle volume scattering cross section
$p(r,\theta)$	Particle scattering phase function

The following sections give the steps of the analyses in greater detail.

3.2 Retrieval of $\gamma(r)$

Of all the equations of Table 1 that define the transverse profiles in terms of radial profiles, Eq. (34), for the particle-only transmittance, is unique because the kernel function G is identically unity. Thus, an immediate Abel inversion of $-\ln \tau_p(z)$ yields the radial volume extinction cross section $\gamma(r)$. That is,

Table 1. E/A Transfer Equations in Cylindrical Coordinates and in Source Function-Kernel

$$\text{Product Form. } F(z) = 2 \int_z^R J(r) G(z, r) \frac{r dr}{(r^2 - z^2)^{1/2}}; \quad G(z, r) = \frac{1}{2} [G^+(z, r) + G^-(z, r)] .$$

Eq.	$F(z)$	$J(r)$	$G^\pm(z, r)$
31	$\bar{N}(z)$	$\bar{\kappa}(r) B_g(r)$	$\tau_\alpha^\pm(z, r) \tau_\beta^\pm(z, r) \bar{\tau}^\pm(z, r) \left[y^\pm(z, r) + \frac{J(r) + Q_S^\pm(z, r)}{J_g(r)} \right]$
32	$-\ln \bar{\tau}(z)$	$\bar{\kappa}(r)$	$\frac{\gamma(r)}{\bar{\kappa}(r)} + y^\pm(z, r)$
33	$N_p(z)$	$\alpha(r) B_p(r)$	$\tau_\alpha^\pm(z, r) \tau_\beta^\pm(z, r) \left[1 + \frac{Q_S^\pm(z, r)}{J_p(r)} \right]$
34	$-\ln \tau_p(z)$	$\gamma(r)$	1
35	$\bar{N}_g(z)$	$\bar{\kappa}(r) B_g(r)$	$y^\pm(z, r) \bar{\tau}^\pm(z, r)$
36	$-\ln \bar{\tau}_g(z)$	$\bar{\kappa}(r)$	$y^\pm(z, r)$

Note: The $Q_S^\pm(z, r)$ appearing in Eqs. 31 and 33 are not the same function. In Eq. 31, $Q_S^\pm(s, r)$ is computed with gas in the scattering lines of sight; in Eq. 33, computation is made with no gas in the scattering lines of sight.

$$\gamma(r) = A[-\ln \tau_p(z)] \quad (48)$$

where A is the Abel inversion operator defined by Eqs. (46) and (47).

3.3 Retrieval of $\alpha(r)$, $\beta(r)$, and $p(r, \theta)$

The second step in the retrieval involves an iterative Abel inversion of the laser scattering function $f(z, \theta)$ for each θ to obtain $J(r, \theta) = \beta(r) p(r, \theta)/4\pi$ [see Eqs. (42) and (43)]. That is

$$J(r, \theta) = \frac{\beta(r) p(r, \theta)}{4\pi} = IA [f(z, \theta)] \quad (49)$$

where IA is the iterative Abel inversion operator defined by the procedure of Fig. 4. The iteration initiation assumption $G = 1$ is equivalent to the assumption that the plume is nonscattering. Integration of this result over all solid angles yields

$$\int_{4\pi} J(r, \theta) d\Omega = \frac{\beta(r)}{4\pi} \int_{4\pi} p(r, \theta) d\Omega = \beta(r) \quad (50)$$

since the phase function is normalized to 4π . With the volume scattering cross section $\beta(r)$ now known, the volume attenuation cross section $\alpha(r)$ can be obtained from

$$\alpha(r) = \gamma(r) - \beta(r), \quad (51)$$

and the scattering phase function from

$$p(r, \theta) = \frac{4\pi}{\beta(r)} J(r, \theta). \quad (52)$$

For some applications, it may be reasonable to assume that α , β , and $p(\theta)$ to not depend on radius. In this case, the line-of-sight equation [Eq. (42)] reduces to

$$f(z, \theta) = \frac{\beta}{4\pi} p(\theta) 2 \int_z^R G(z, r, \theta) \frac{r dr}{(r^2 - z^2)^{1/2}} \quad (53)$$

and $\beta p(\theta)$ can be obtained directly from data taken for a single transverse value z (presumably $z = 0$ for best signal) without inversion by

$$J(\theta) = \frac{\beta}{4\pi} p(\theta) = \frac{f(z, \theta)}{2 \int_z^R G(z, r, \theta) \frac{r dr}{(r^2 - z^2)^{1/2}}} \quad (54)$$

As for the general case, an integration over all solid angles allows for a determination of β (and thus α) and $p(\theta)$ individually. The consequences of this simplification to the diagnostic itself are not great since the iterative Abel inversion for the general case is easy to implement and is fast. A significant simplification to experimental measurement would be effected, however, since now the laser source would not have to be traversed in z .

3.4 Retrieval of $T_p(r)$

The particle temperature profile is retrieved by iterative Abel inversion on the particle-only radiance profile. The retrieved source function is [see Eq. (33), Table 1].

$$\alpha(r) B_p(r) = I_A [N_p(z)]. \quad (55)$$

With $\alpha(r)$ known, $B_g(r)$ and thus $T_p(r)$ can be found. The iteration initiation assumption $G = 1$ for this inversion is equivalent to the assumption that the plume is nonscattering.

At this point, all of the particle properties that are required for further analysis, or for radiation calculations in general, have been obtained.

3.5 Retrieved of $T_g(r)$ and $\bar{\kappa}(r)$

The retrieval for gas temperature T_g and volume gas absorption cross section $\bar{\kappa}$ proceeds by a simultaneous iterative Abel inversion on the total gas-particle emission and absorption profiles [Eqs. (31) and (32), Table 1]. The need for a simultaneous solution is that the emission and transmission profiles are coupled through the dependence of $\bar{\kappa}$ on T_g . This coupling did not occur in the particle-only retrieval of T_p and γ because γ can be obtained in a single Abel inversion. The retrieved source functions are

$$\begin{Bmatrix} \bar{\kappa}(r) B_g(r) \\ \bar{\kappa}(r) \end{Bmatrix} = \text{IA} \begin{Bmatrix} \bar{N}(z) \\ \bar{\tau}(z) \end{Bmatrix} . \quad (56)$$

The retrieval of the gas temperature $T_g(r)$ and the gas concentration $c_g(r)$ from these two source functions is described in Ref. 1. The initiation assumption $G = 1$ for the iterative Abel inversion is equivalent to the assumption that the source is a thin, gas-only plume.

4. APPLICATION

The particle- and gas-property retrieval schemes developed in Section 3 were applied to the minimum smoke propellant (MSP), advanced liquid propellant (ALP), and reduced smoke propellant (RSP) models considered in the previous phase of this work (Ref. 6). In Section 4.1, the flow-field properties of the three plume models are summarized, and in Section 4.2, the computed transverse E/A and laser scattering profiles are discussed. In Sections 4.3 and 4.4, respectively, the particle and gas retrieval results are presented.

4.1 Plume Model Summary

A summary of the plume model parameters is given in Table 2 and the radial temperature and concentrations are shown in Figs. 5-7. The differential scattering cross sections used for the three particle species Al_2O_3 , C, and ZrO_2 are shown in Figs. 8-10. These scattering cross sections (and the cross sections in Table 2) for Al_2O_3 and ZrO_2 were obtained for the bimodal particle size distribution described in Ref. 6. The peaks of the distribution are at particle radii of 0.05 and 0.5 μm . The index of refraction used was $m = 2.0 - 0.01i$ at $\lambda = 2.51 \mu\text{m}$ for Al_2O_3 and $m = 1.2 - 0.01i$ at $\lambda = 3.38 \mu\text{m}$ for ZrO_2 . The scattering cross sections for C were obtained with a size distribution function that peaks at a radius of 0.05 μm and falls by two orders of magnitude by 0.5 μm . The index of refraction used was $m = 2.6 - 1.0i$. The gas band model parameters for H_2O at 2.51 μm and HCl at 3.89 μm are discussed in Ref. 6.

Table 2. Summary of Plume Model Data.

Model	MSP	ALP	RSP ^(a)
$\lambda(\mu\text{m})$	2.51	3.89	2.51
Gas	H ₂ O	HCl	H ₂ O
Particle	Al ₂ O ₃ ^(b)	C	ZrO ₂
R(cm)	10	7	5.69
c (mole fraction)	0.15	0.117	0.155
p (atm)	1.0	1.18	---
n_p (cm ⁻³)	10 ⁵	1.37 x 10 ⁸	---
σ_a (cm ²)	3.20 x 10 ⁻⁹	4.62 x 10 ⁻¹⁰	1.41 x 10 ⁻⁹
σ_s (cm ²)	5.86 x 10 ⁻⁸	2.17 x 10 ⁻¹⁰	8.41 x 10 ⁻⁹
L ₁ (cm)	3.0	2.5	3.0
L ₂ (cm)	57	83	44
T _N (K)	800	1500	1460
ϵ_N	0.75	0.25	0.25

λ wavelength
R plume radius
c gas concentration
p total gas pressure
 n_p particle loading
 σ_a absorption cross section
 σ_s scattering cross section
L₁ exit plane - observation plane distance
L₂ observation plane - end plane distance
T_N nozzle temperature
 ϵ_N nozzle emissivity

(a) Low-temperature model of Ref. 6.

(b) With imaginary index $\kappa = 0.01$.

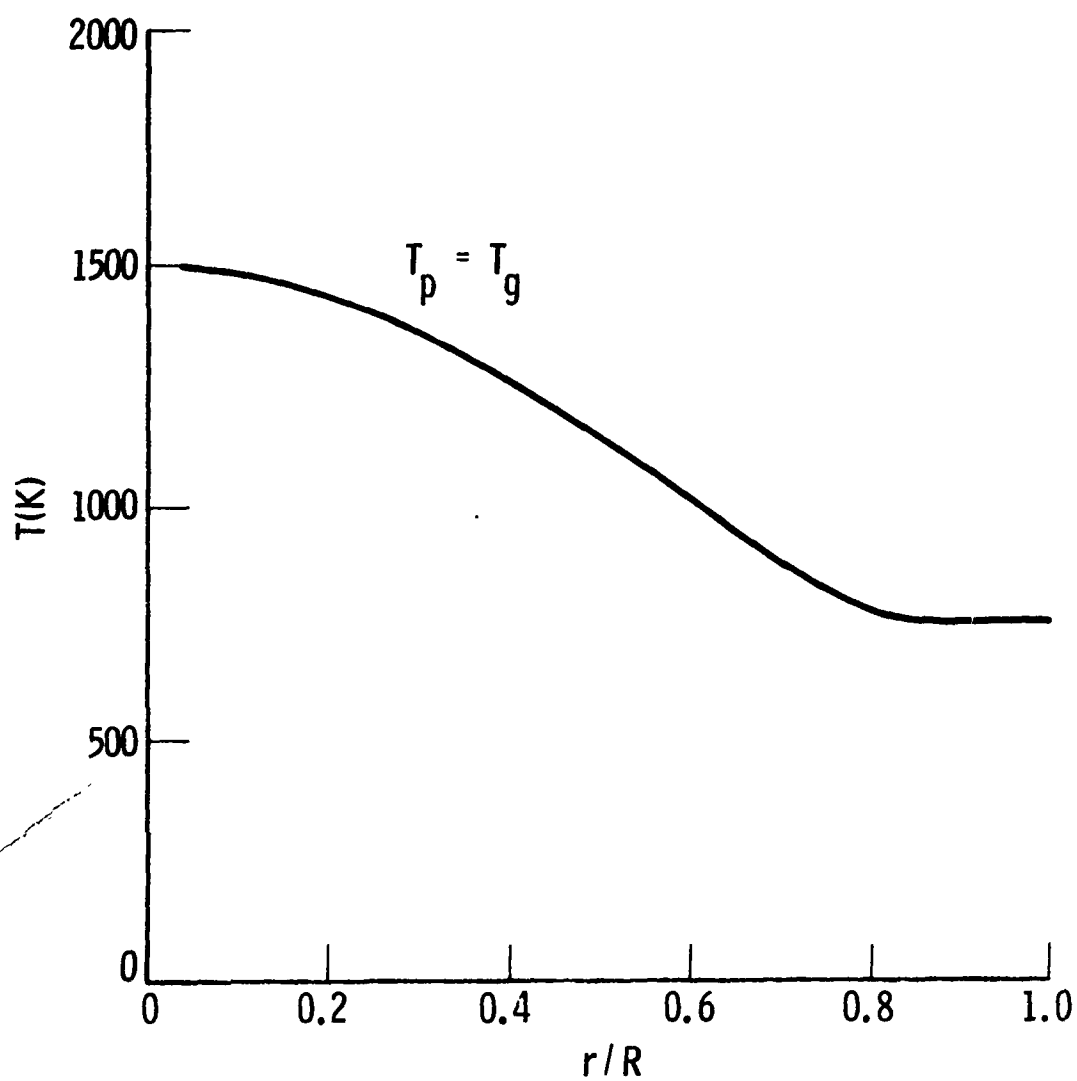


Fig. 5. Radial Temperature Profiles for the MSP Plume Model.

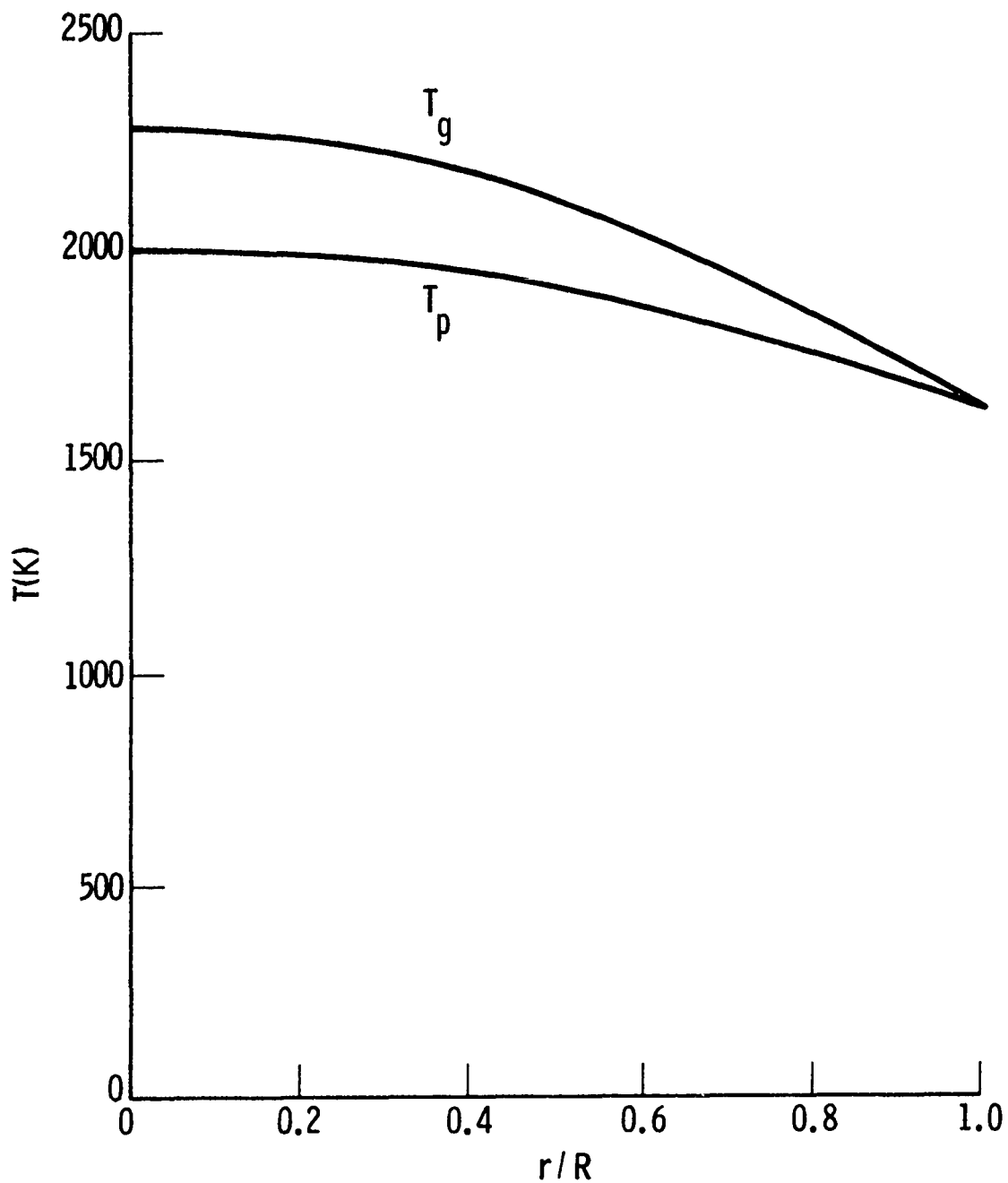


Fig. 6. Radial Temperature Profiles for the ALP Plume Model.

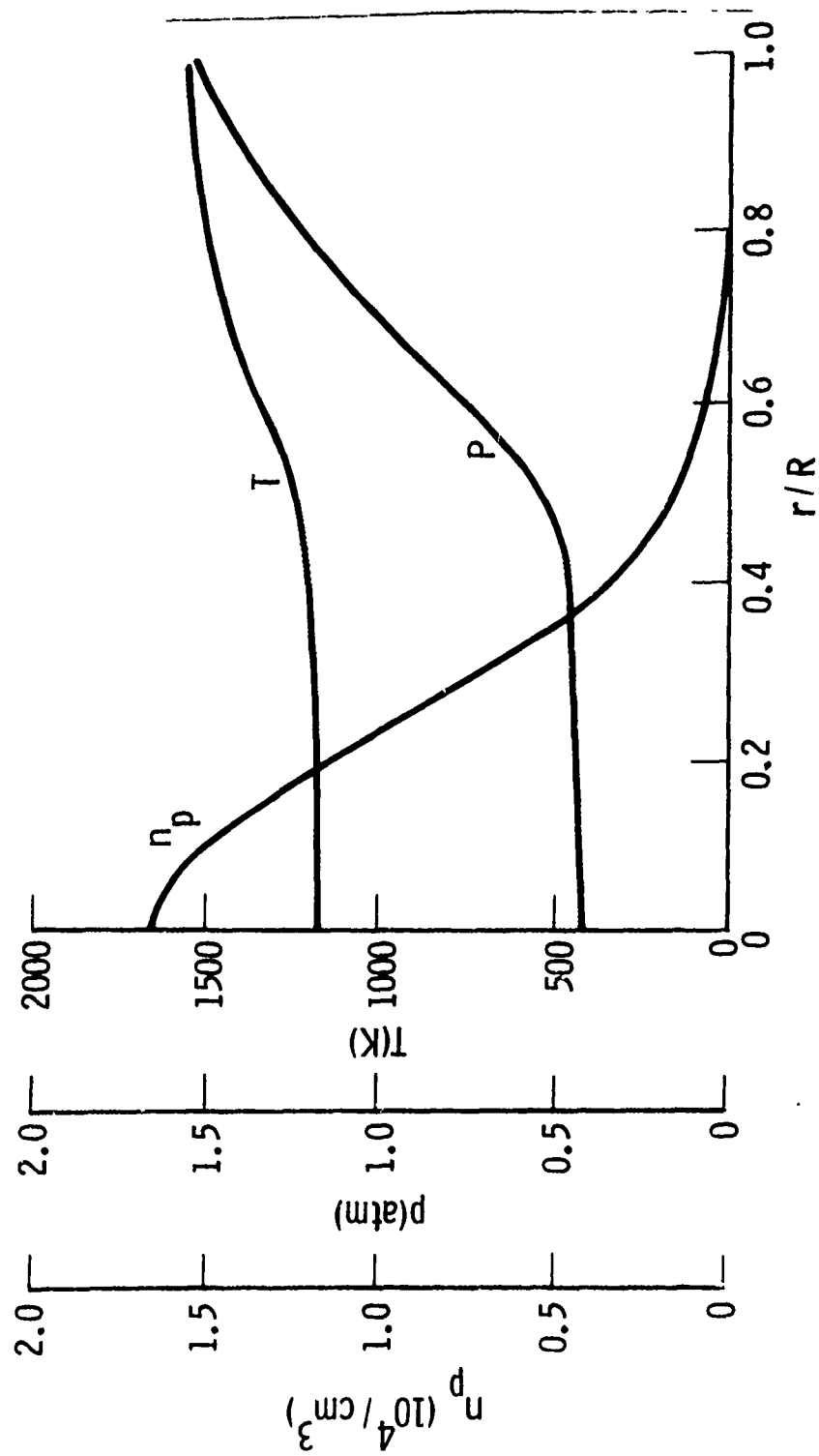


Fig. 7. Radial Profiles for the RSP Plume Model.

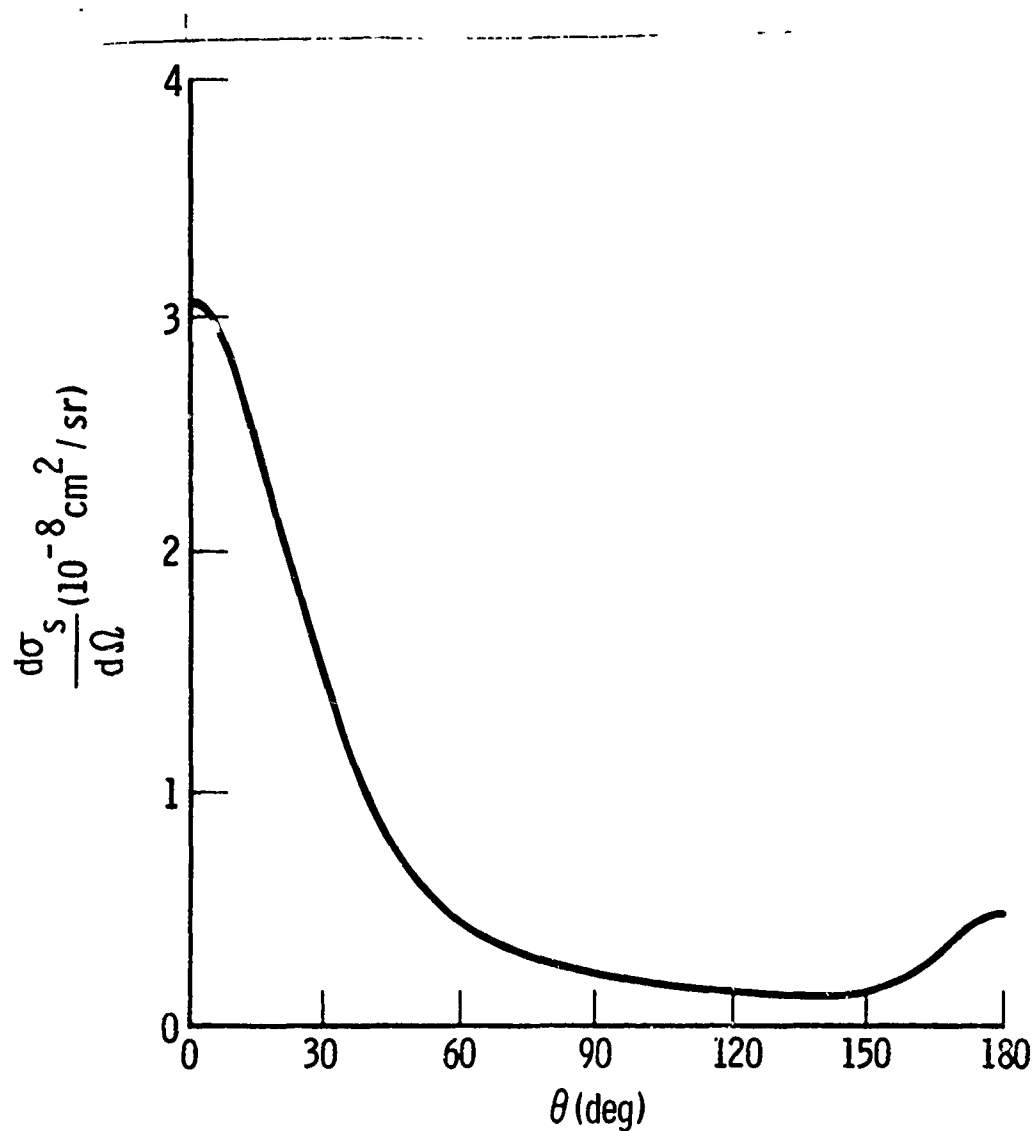


Fig. 8. Differential Scattering Cross Section for Al_2O_3 .

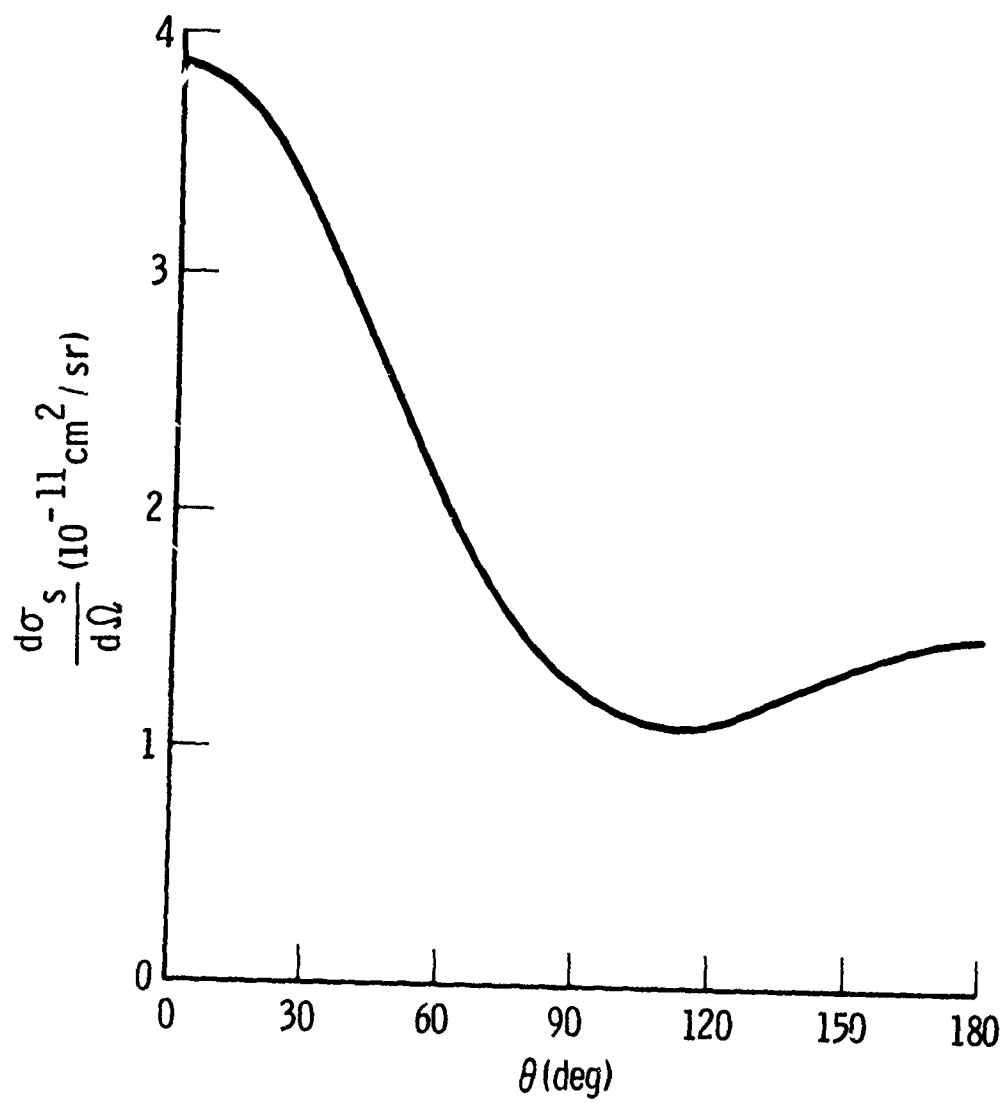


Fig. 9. Differential Scattering Cross Section for C.

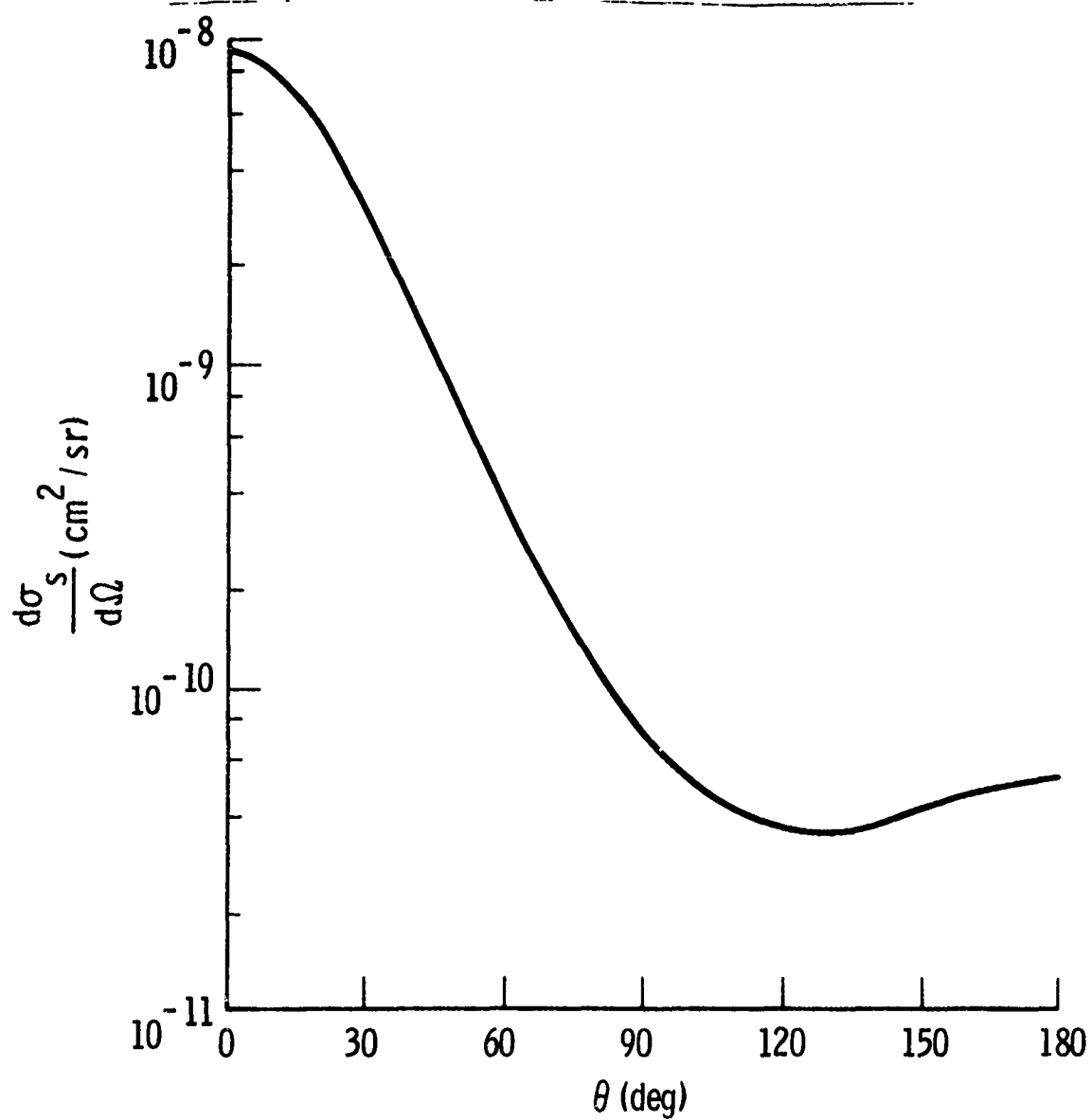


Fig. 10. Differential Scattering Cross Section for ZrO₂.

4.2 Emission/Attenuation Profiles and Laser Scattering Results

For all three cases, transverse profile calculations were performed for a Lorentz lineshape and the Curtis-Godson nonuniformity approximation. For numerical integration along the observation lines of sight, the plume was divided into 10 annular zones. Integrations along scattering lines of sight employed a grid of 10 equal-size intervals. Angular integration was performed with the 11-point scattering angle grid $\theta = 0, 5, 15, 25, 35, 45, 60, 90, 120, 150$ and 180° and an azimuthal grid of 16 equal-size intervals ($\Delta\phi = 22.5^\circ$). The laser scattering function $f(z, \theta)$ was computed on the 8-point grid $\theta_L = 0, 10, 20, 30, 45, 90, 135, \text{ and } 180^\circ$.

The computed transverse profiles for total gas-particle radiance and transmittance are shown in Figs. 11-16, and duplicate the results of Ref. 6. The MSP and RSP models represent plumes whose radiation and attenuation are, for the most part, dominated by the gas component of the plume. In the ALP model, however, particles play the dominant role. The loading of the ALP model is so large, in fact, that the condition of signal-scattering required by the radiation model is most assuredly violated, and neither the radiation nor the extinction results for this model should be believed. However, the results can be used to test the inversion procedures because the same single-scattering model is employed in the inversion.

Representative scattering efficiency function results are given in Figs. 17-22. The angular variation of these functions essentially reflect the angular variation of the particle scattering phase functions (Figs. 8-10). (Note, however, that these functions are not required to be symmetric at $\theta = 0$ and 180° , while the phase functions are.) The overall decrease in magnitude of the angular variation with increasing z is caused by the decreased scattering path length and the increased amount of plume that the

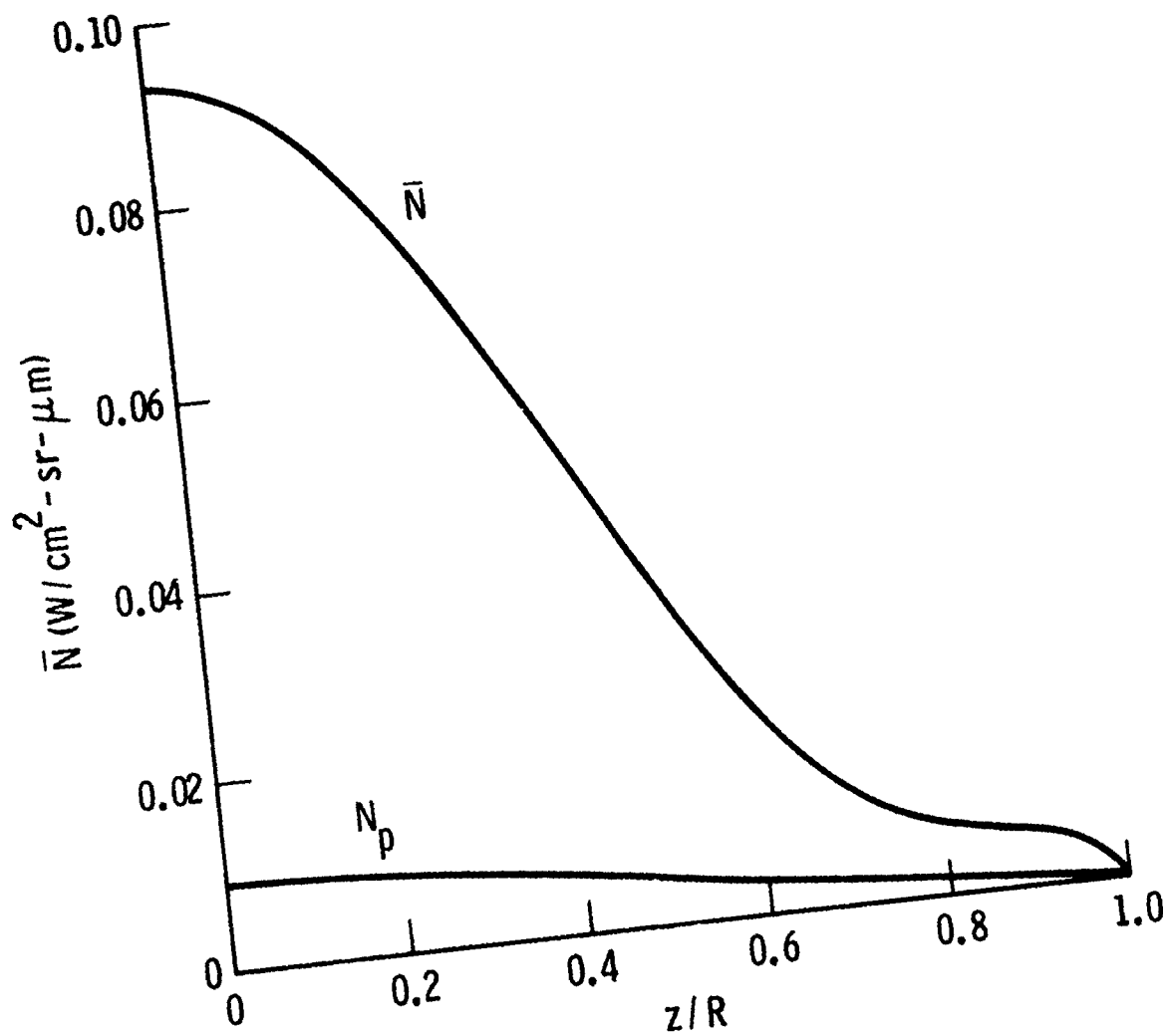


Fig. 11. Transverse Radiance Profiles for the MSP Plume Model.

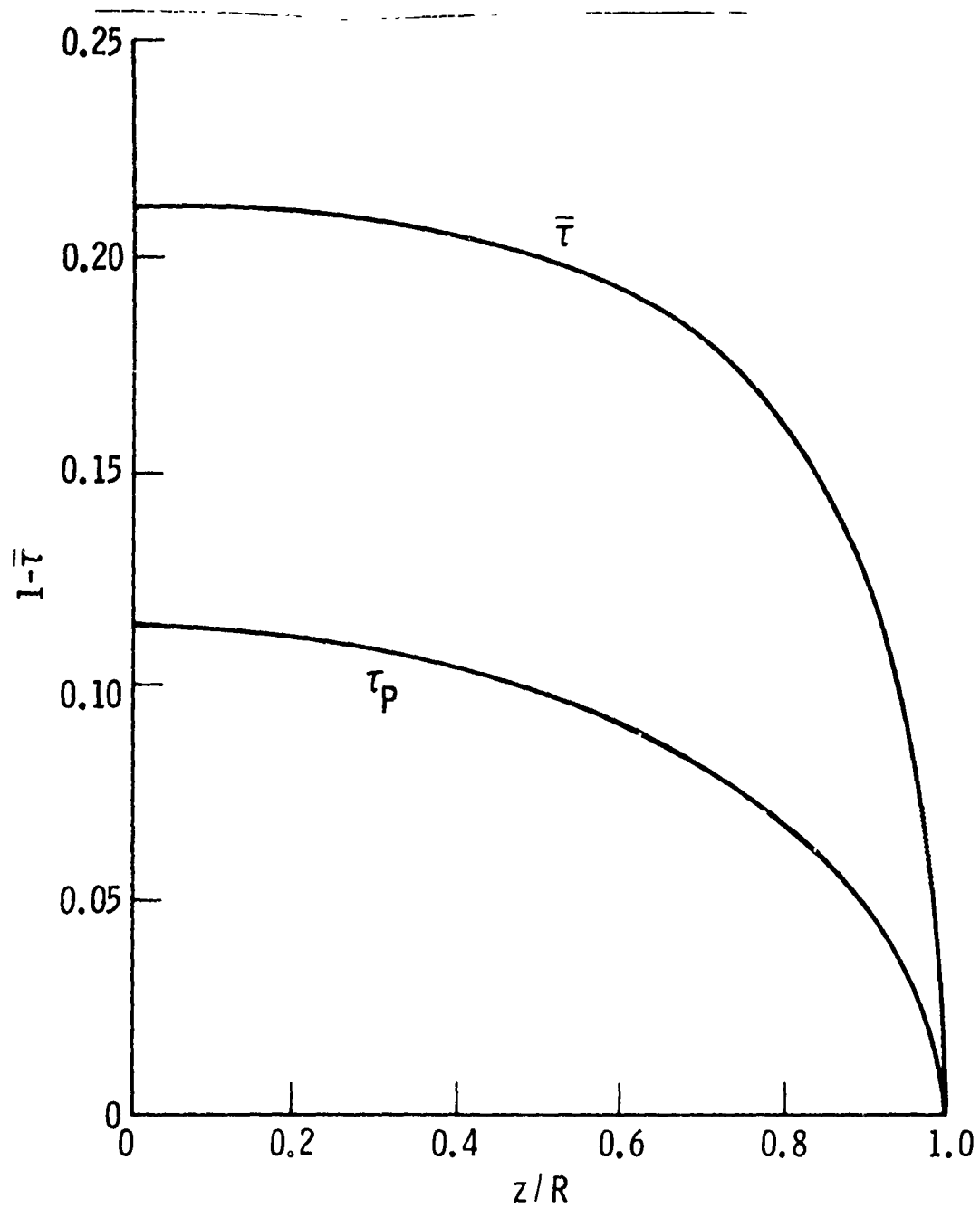


Fig. 12. Transverse Extinctance Profiles for the MSP Plume Model.

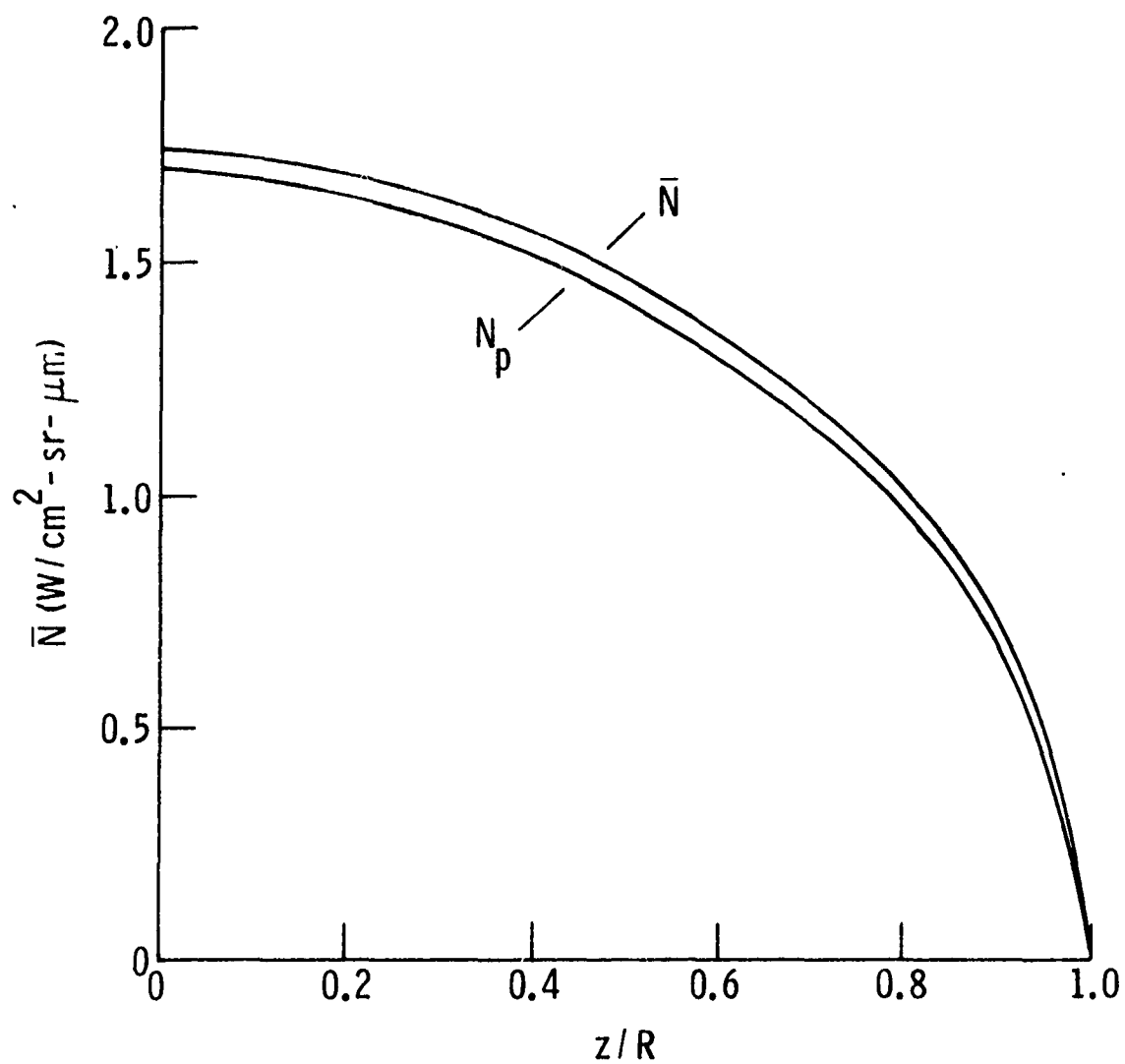


Fig. 13. Transverse Radiance Profiles for the ALP Plume Model.

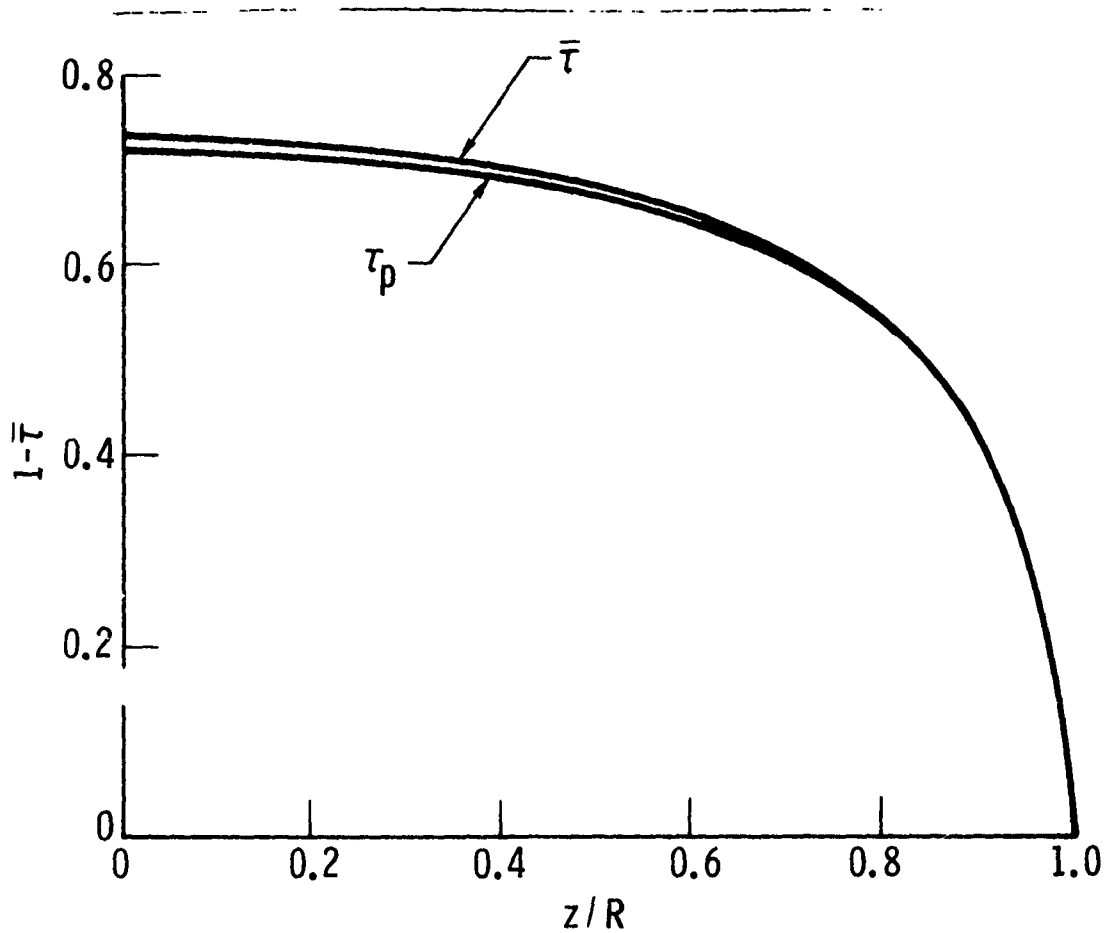


Fig. 14. Transverse Extinctance Profiles for the ALP Plume Model.

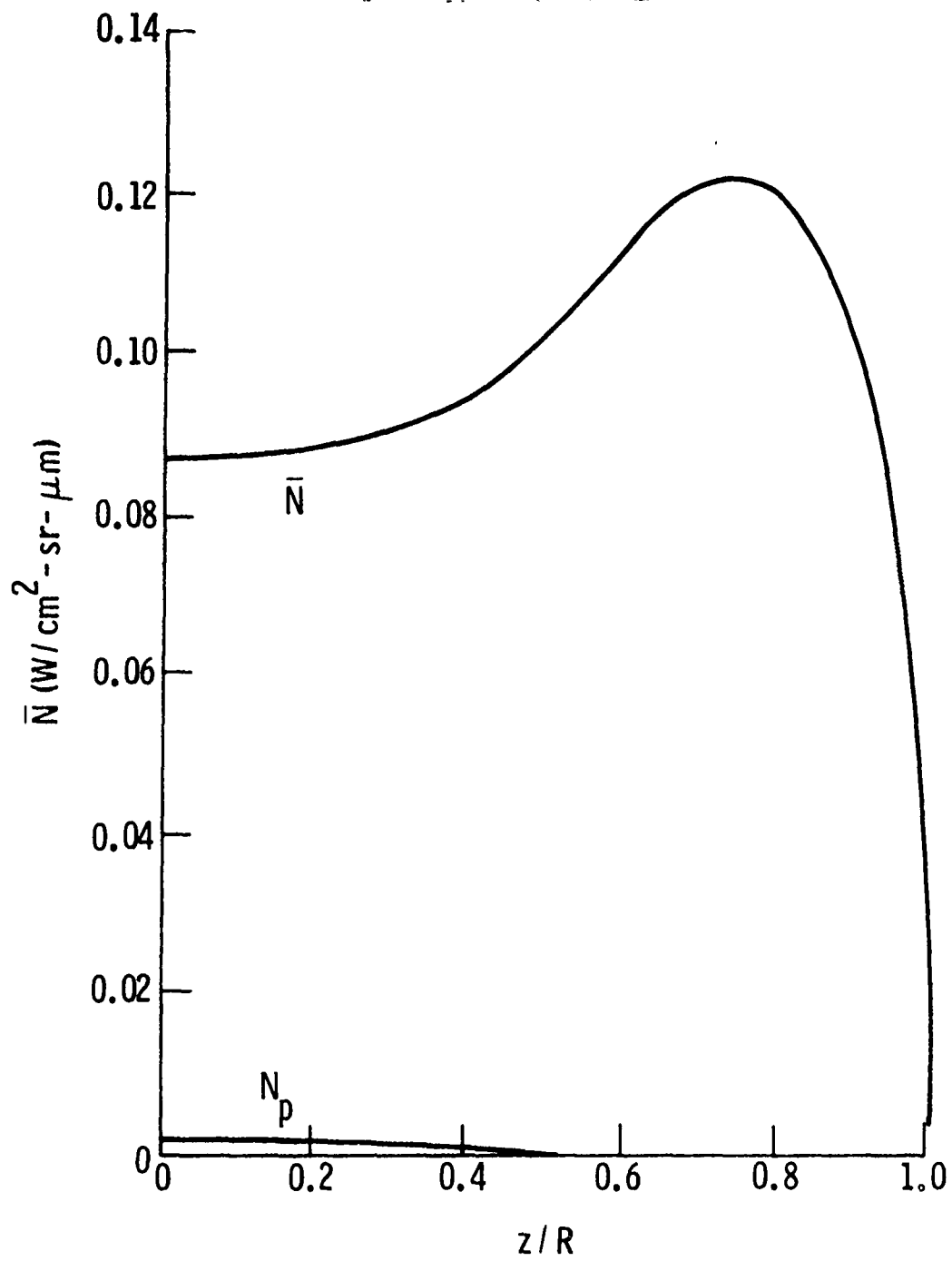


Fig. 15. Transverse Radiance Profiles for the RSP Plume Model.

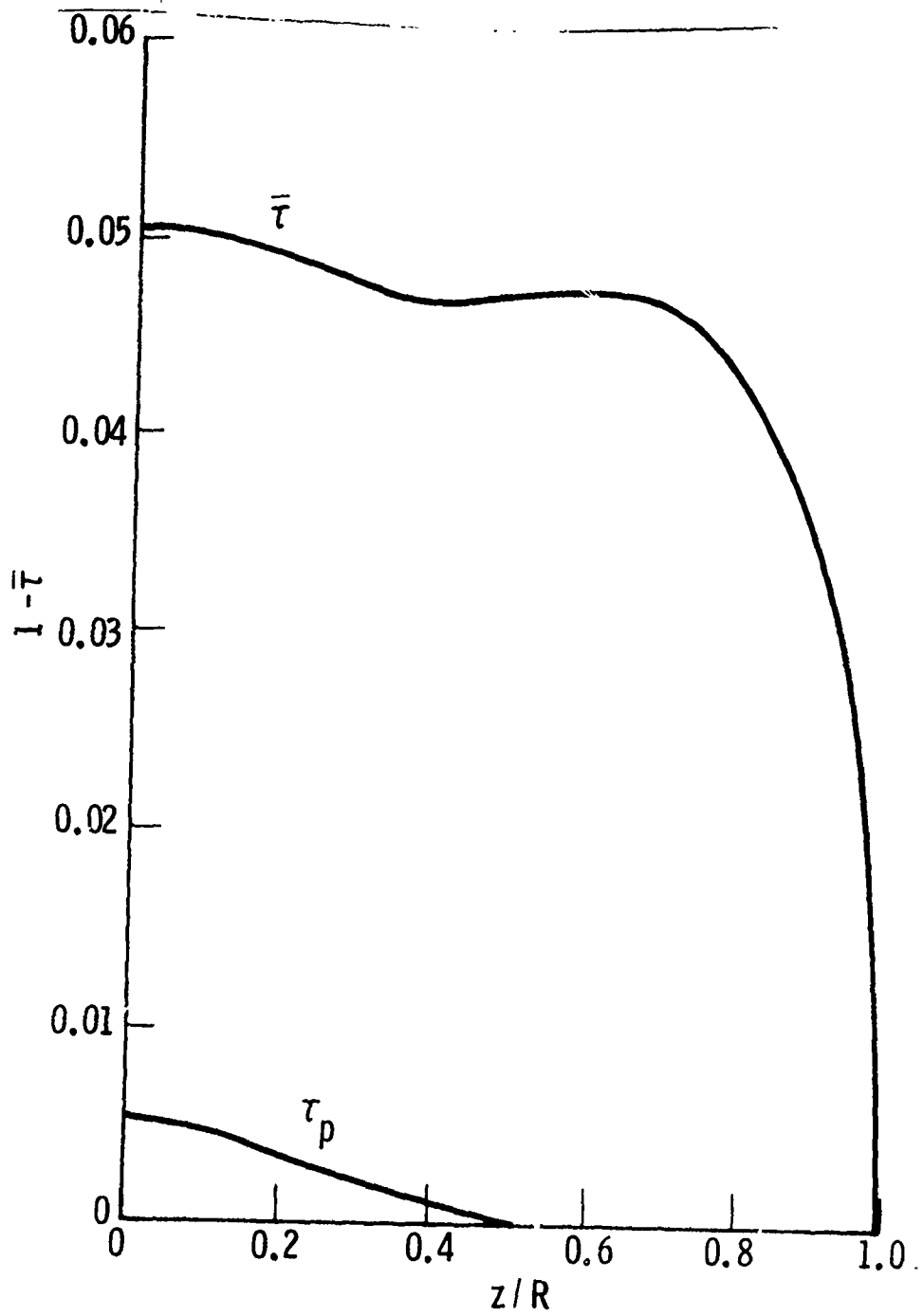


Fig. 16. Transverse Extinctance Profiles for the RSP Plume Model

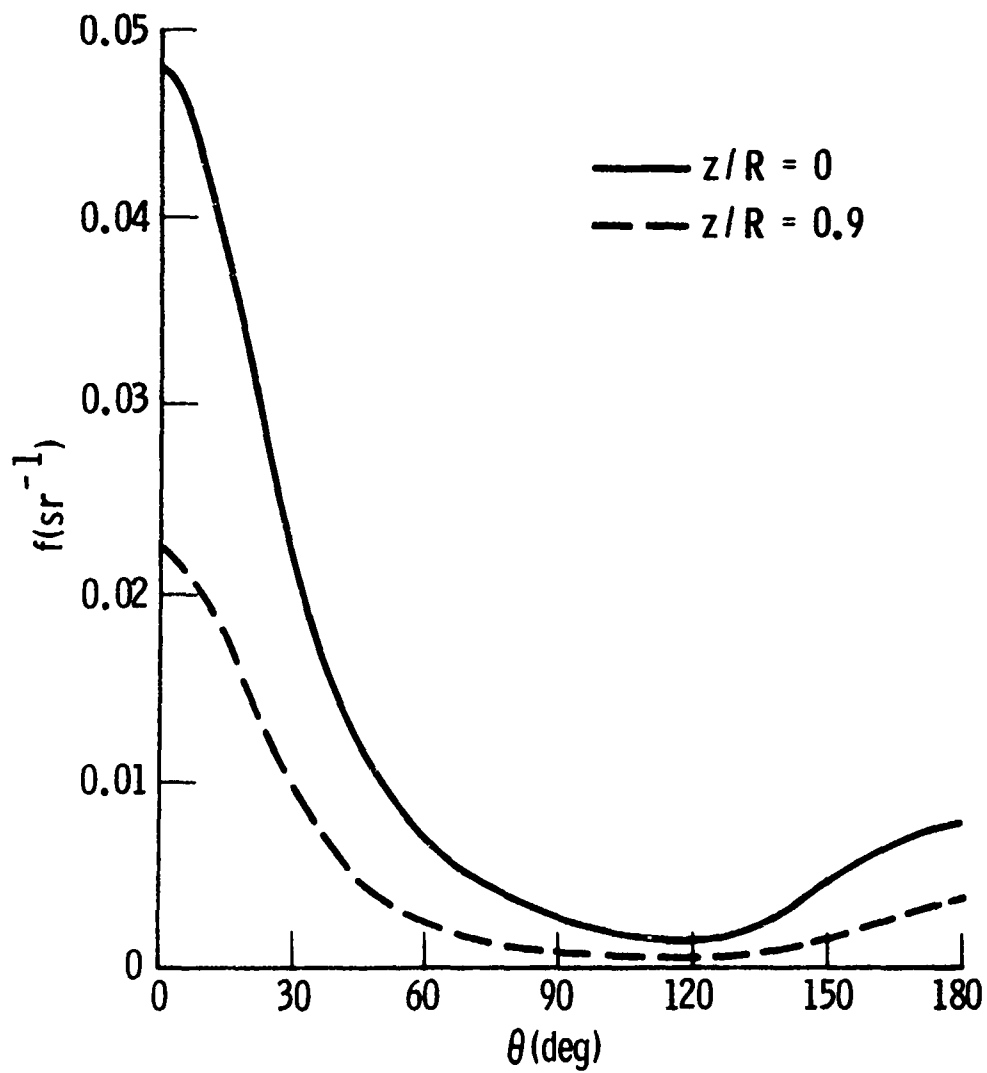


Fig. 17. Angle Variation of Scattering Efficiency Function for the MSP Plume Model

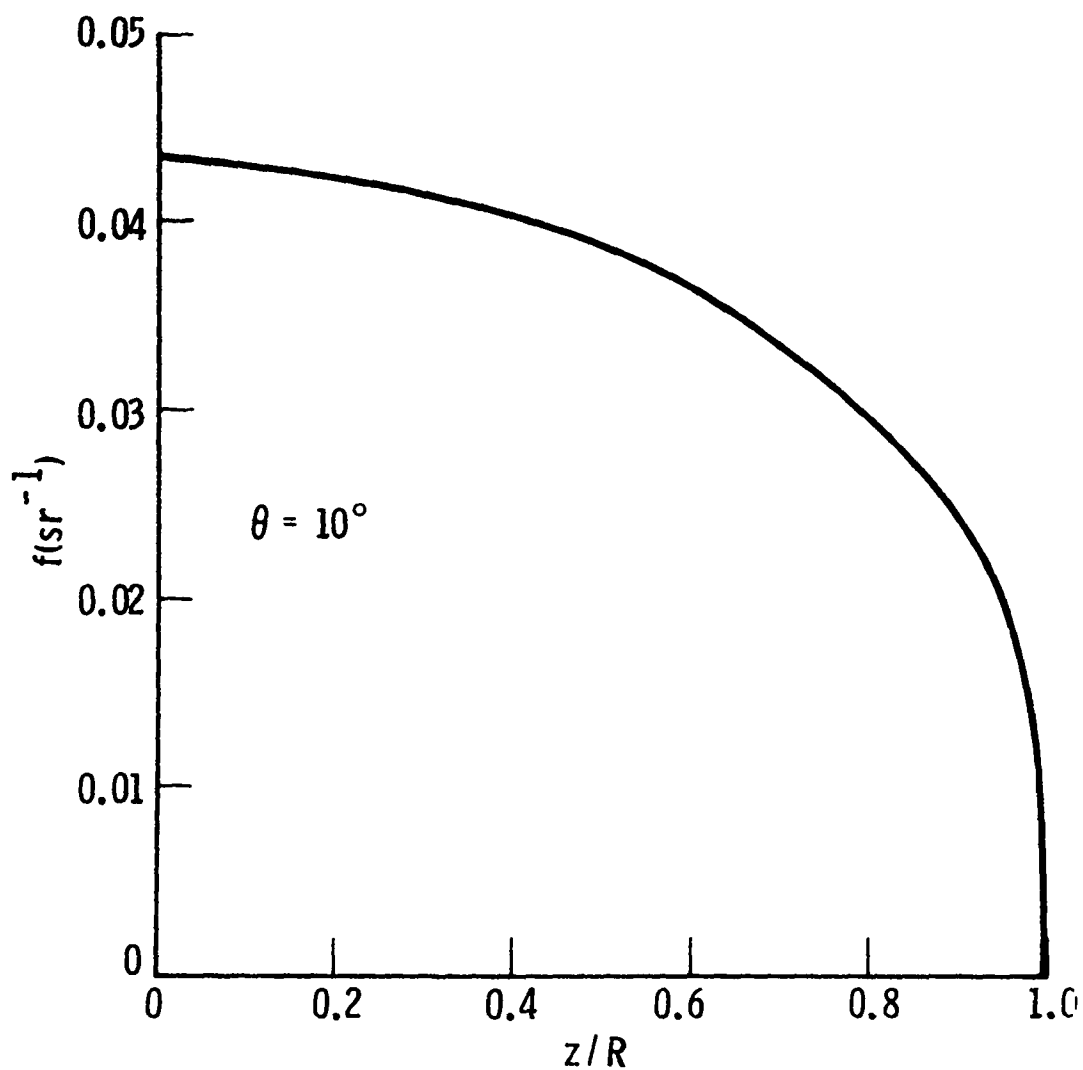


Fig. 18. Transverse Variation of Scattering Efficiency Function for the MSP Plume Model

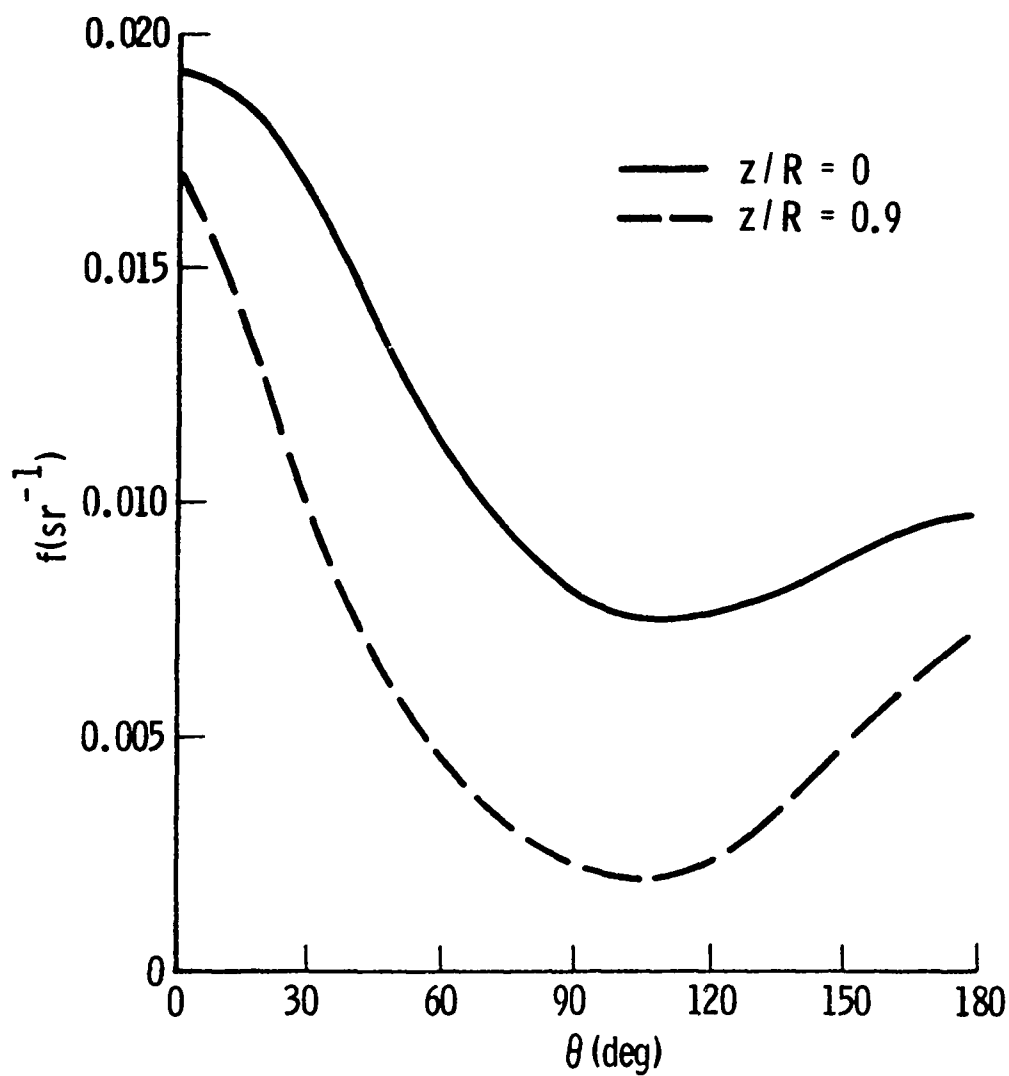


Fig. 19. Angle Variation of Scattering Efficiency Function for the ALP Plume Model

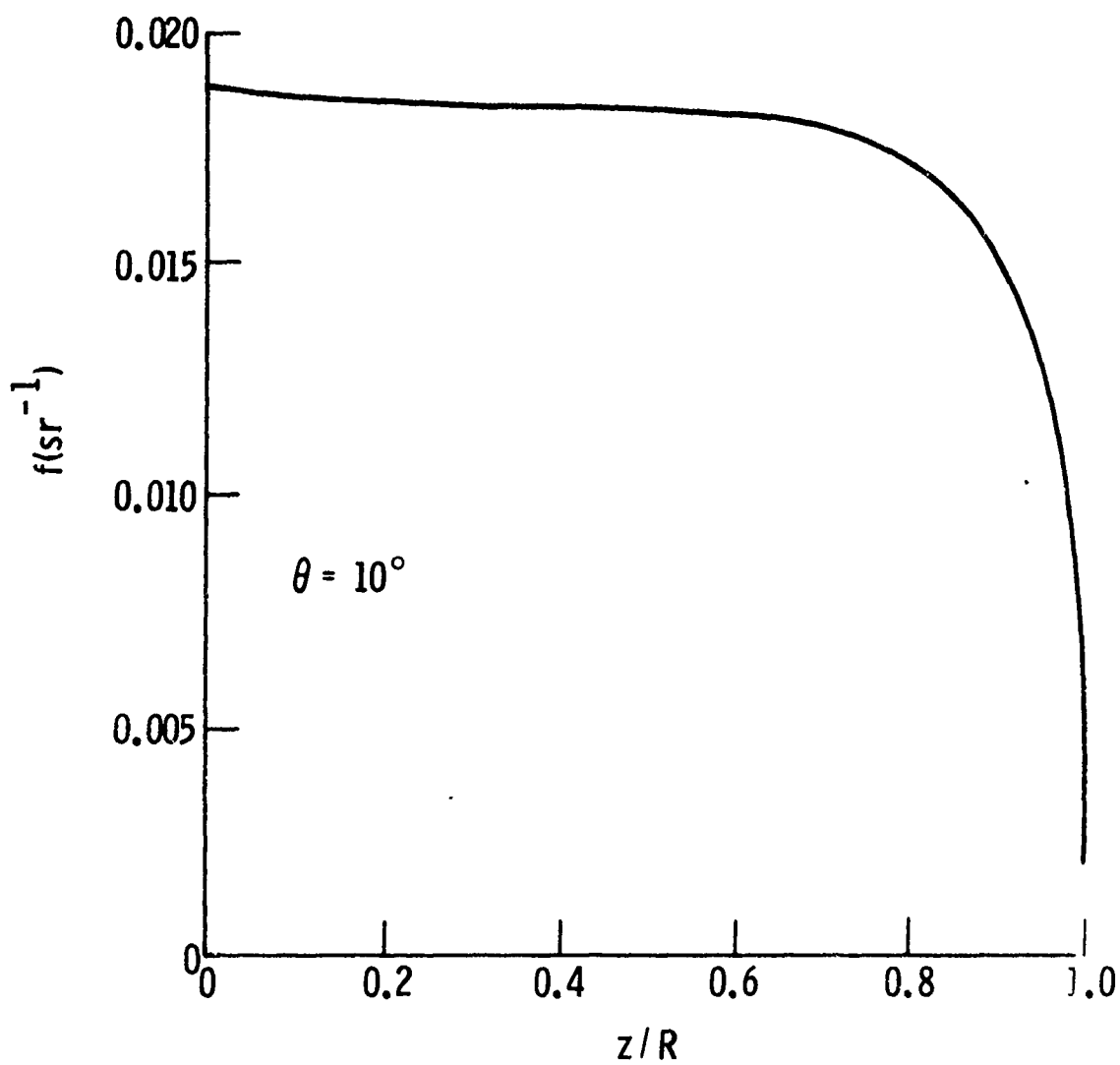


Fig. 20. Transverse Variation of Scattering Efficiency Function for the ALP Plume Model

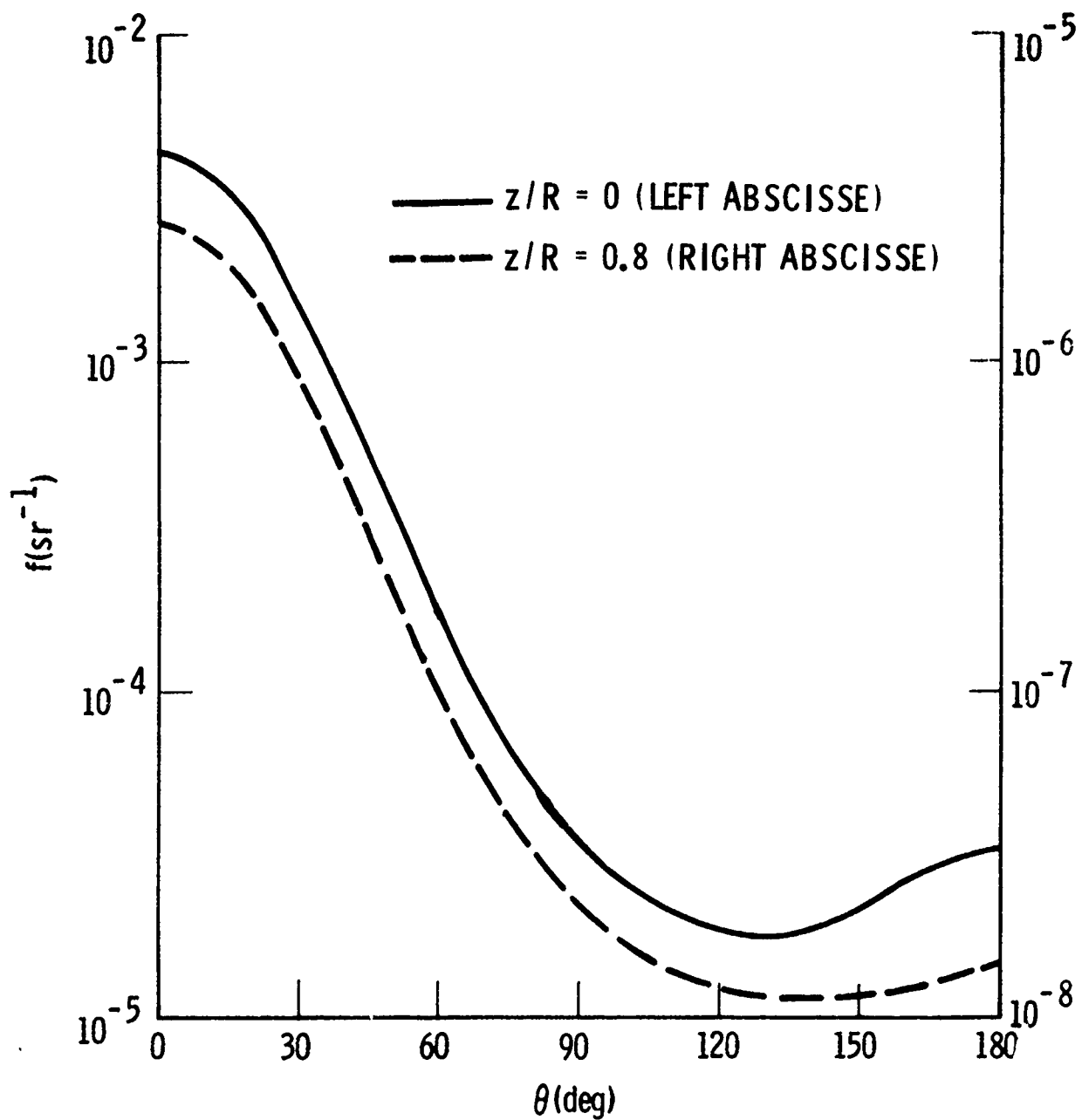


Fig. 21. Angle Variation of Scattering Efficiency Function for the RSP Plume Model

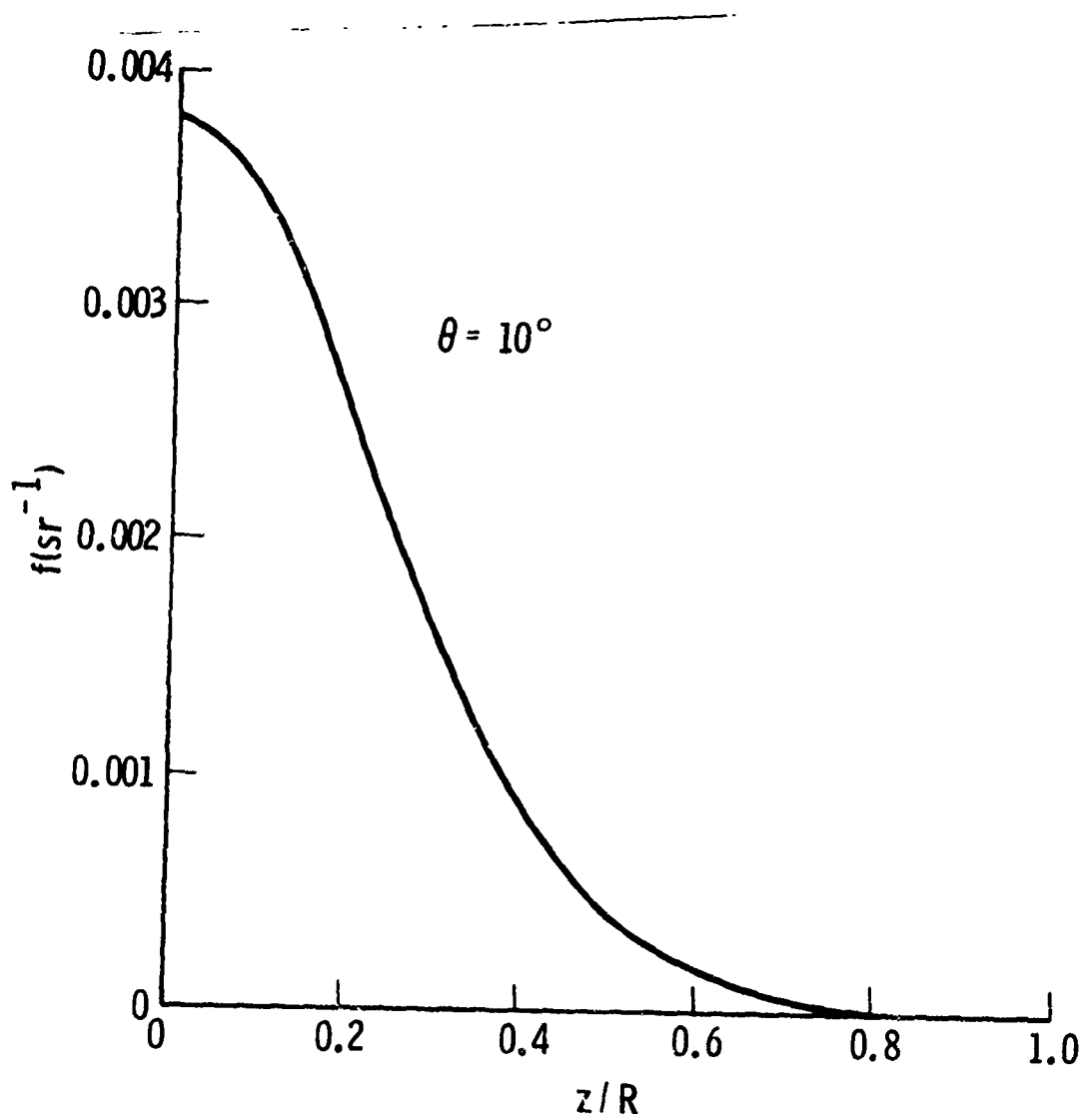


Fig. 22. Transverse Variation of Scattering Efficiency Function for the RSP Plume Model

scattered radiation must pass through before reaching the sensor. In the RSP model (Fig. 21), the decrease in magnitude is further enhanced by the rapid decrease in particle density with radius (Fig. 7).

The E/A and scattering results of Figs. 11-22 are the simulated experimental data to which the inversion algorithms are applied in the following two sections.

4.3 Particle Retrieval Results

For each of the three models, retrieval was made for $\gamma(r)$, $\beta(r)$, $\alpha(r)$, $p(r,\theta)$ and $T_p(r)$ as described in Section 3.* All of the computation conditions used to generate the transverse profiles (e.g., angle grids and number of zones) were duplicated in the inversions. For the retrieval of $p(r,\theta)$ and $T_p(r)$, which require iteration, the convergence requirement imposed was that the radial root-mean-square difference between successive iterations for the respective source functions be less than or equal to 0.1%.

In all cases but one, the retrieved radial profiles and phase functions were exact to within the convergence criterion. The one exception was the RSP plume model. Here, the retrieval was exact near the plume center, but became increasingly noisy in the outer zones of the plume. In the outermost zone, in fact, retrieved volume cross sections became negative, and retrieval for T_p was indefinite. The retrieval errors are shown in Fig. 23. The cause of the errors is the extreme sparseness of particles in the outer regions of the plume (Fig. 7), and as such is not particularly significant. The large errors

* For comparison with input data, $\gamma = n_p (\sigma_a + \sigma_s)$, $\beta = n_p \sigma_s$, $\alpha = n_p \sigma_a$, and $p(\theta) = (4\pi/\sigma_s) d\sigma_s/d\Omega$.

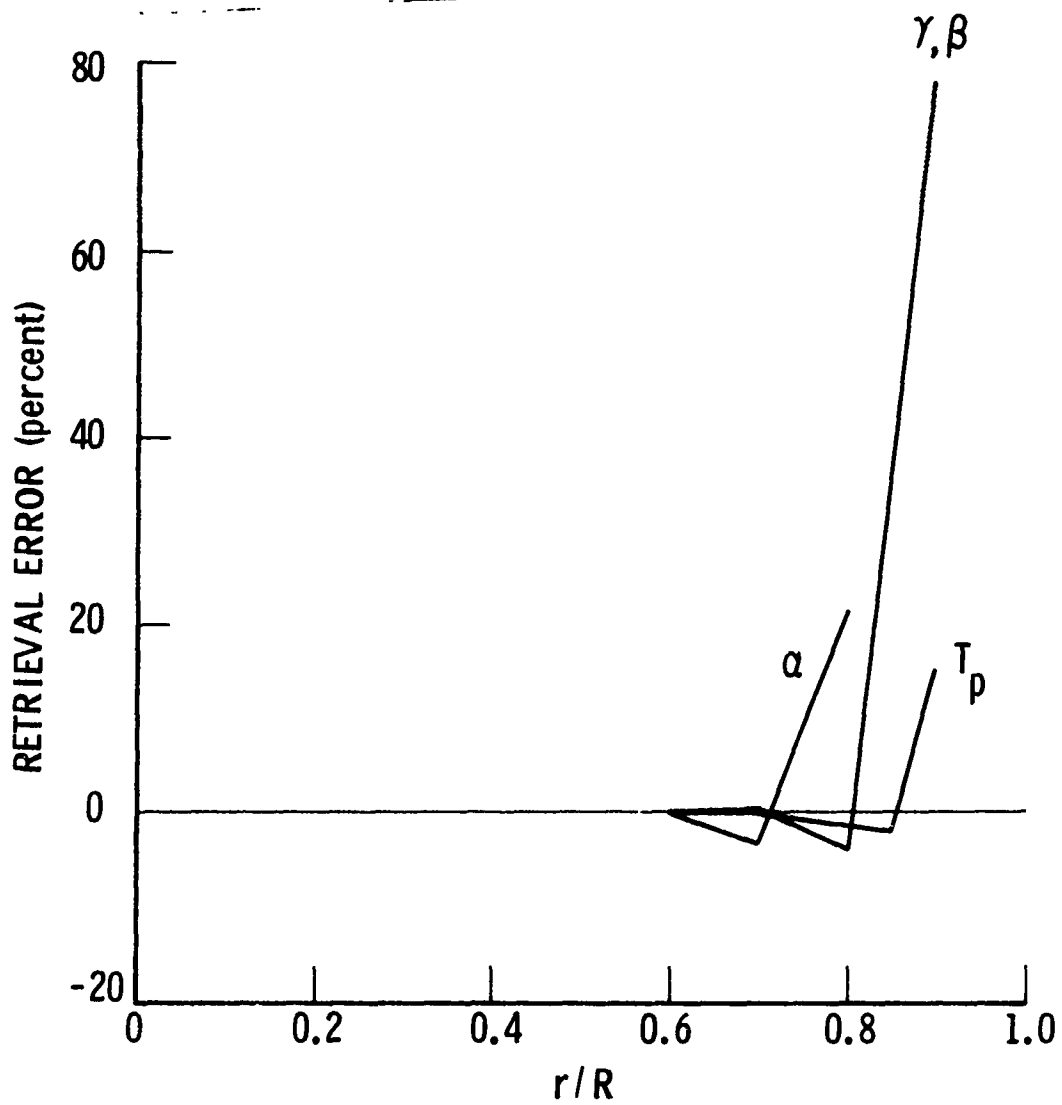


Fig. 23. Particle Properties Retrieval Errors for the RSP Plume Model

merely reflect the fact that we cannot recover the properties of nonexistent (or nearly so) particles.

4.4 Gas Retrieval Results

For each of the three plume models, retrieval was made for gas temperature and concentration using the gas-only and first-order, off-band correction procedures described in Ref. 6, and the fully-coupled gas-plus-particle procedure developed here in Section 3. In the gas-only procedure, the transverse profiles of \bar{N} and $\bar{\tau}$ were treated as if they arose from a purely gaseous plume and used directly as input in a gas-only inversion. In the first-order, off-band correction procedure, a gas-only inversion was made on the profiles $\bar{N} - N_p$ and $\bar{\tau}/\tau_p$. The results of these inversions are shown in Figs. 24-29. The results tabled GAS are the gas-only inversion results, and the results labeled FO/OB are those obtained with the first-order, off-band correction procedure. For the RSP model, the FO/OB results are indistinguishable from the true profiles. The inversions were performed with the same computation conditions (e.g. lineshape and number of zones) used to generate the transverse profiles and with the convergence criteria that the radial root-mean-square difference between iteration results for T_g and c_g should be less than or equal to 0.1%. These inversion results duplicate the results obtained in Ref. 6.

The results of the fully-coupled inversion are not shown explicitly in Figs. 24-29. In all cases, the recovered radial profiles were within the convergence criteria and are indistinguishable from the true profiles when plotted.

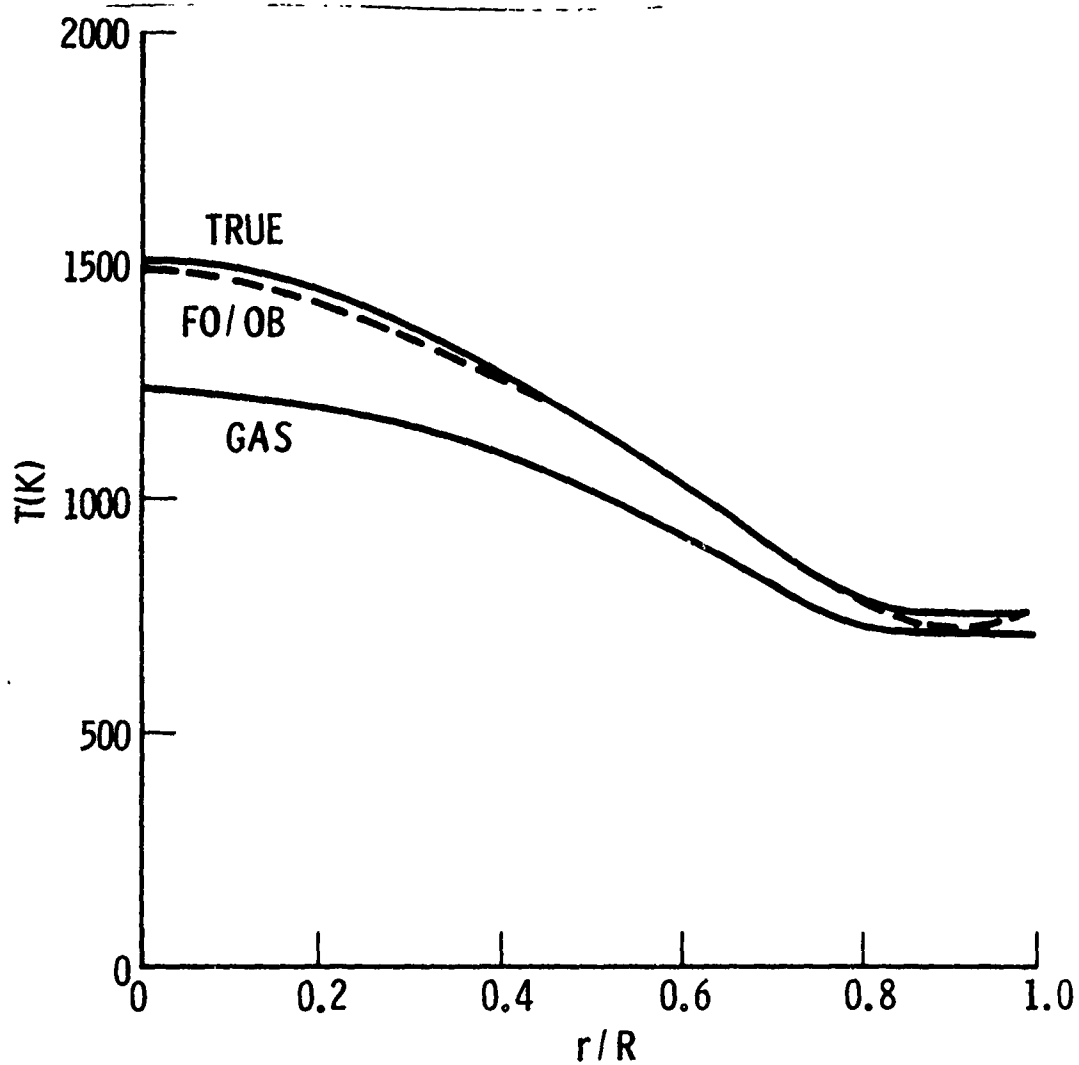


Fig. 24. Gas Temperature Retrieval Results for the MSP Plume Model

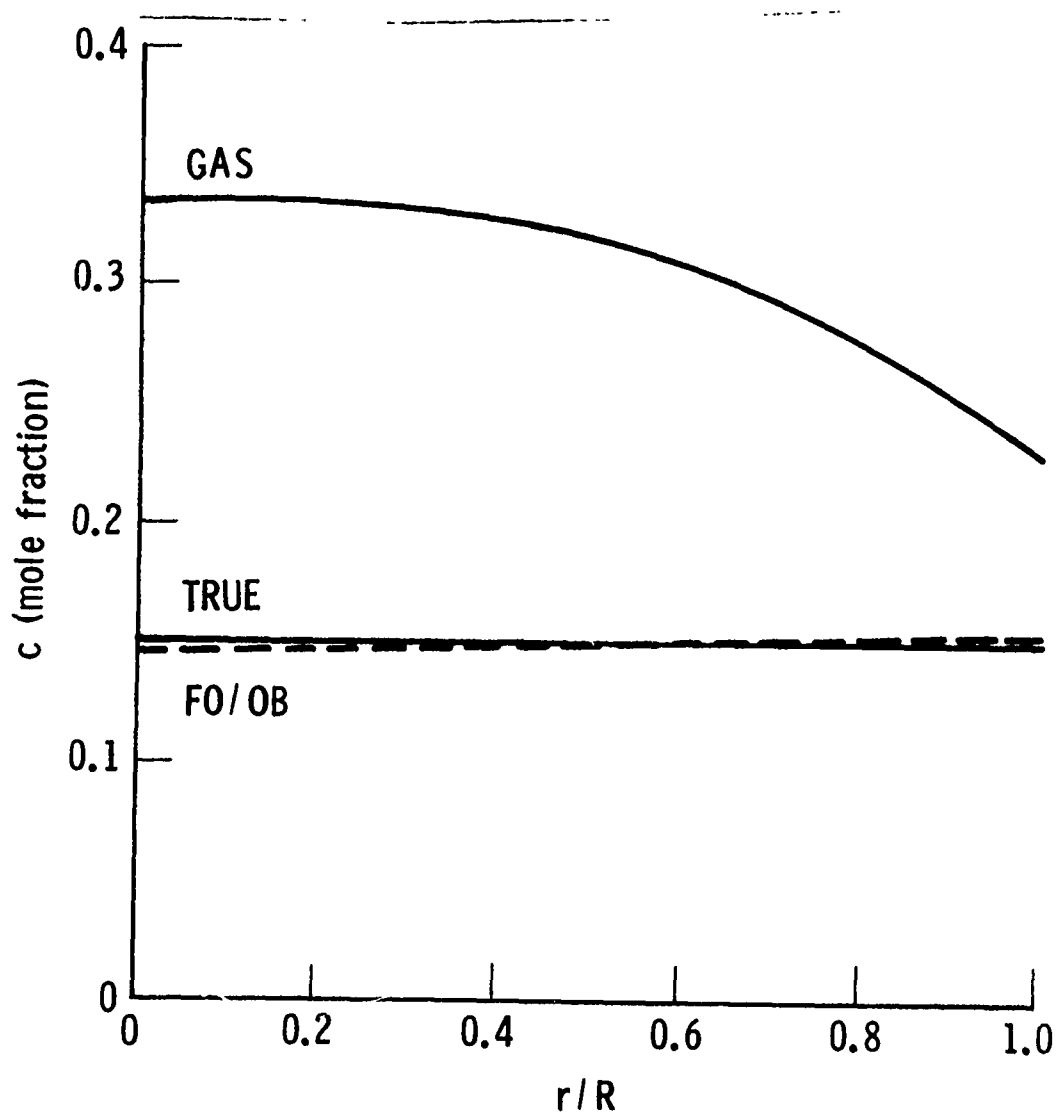


Fig. 25. Gas Concentration Retrieval Results for the MSP Plume Model

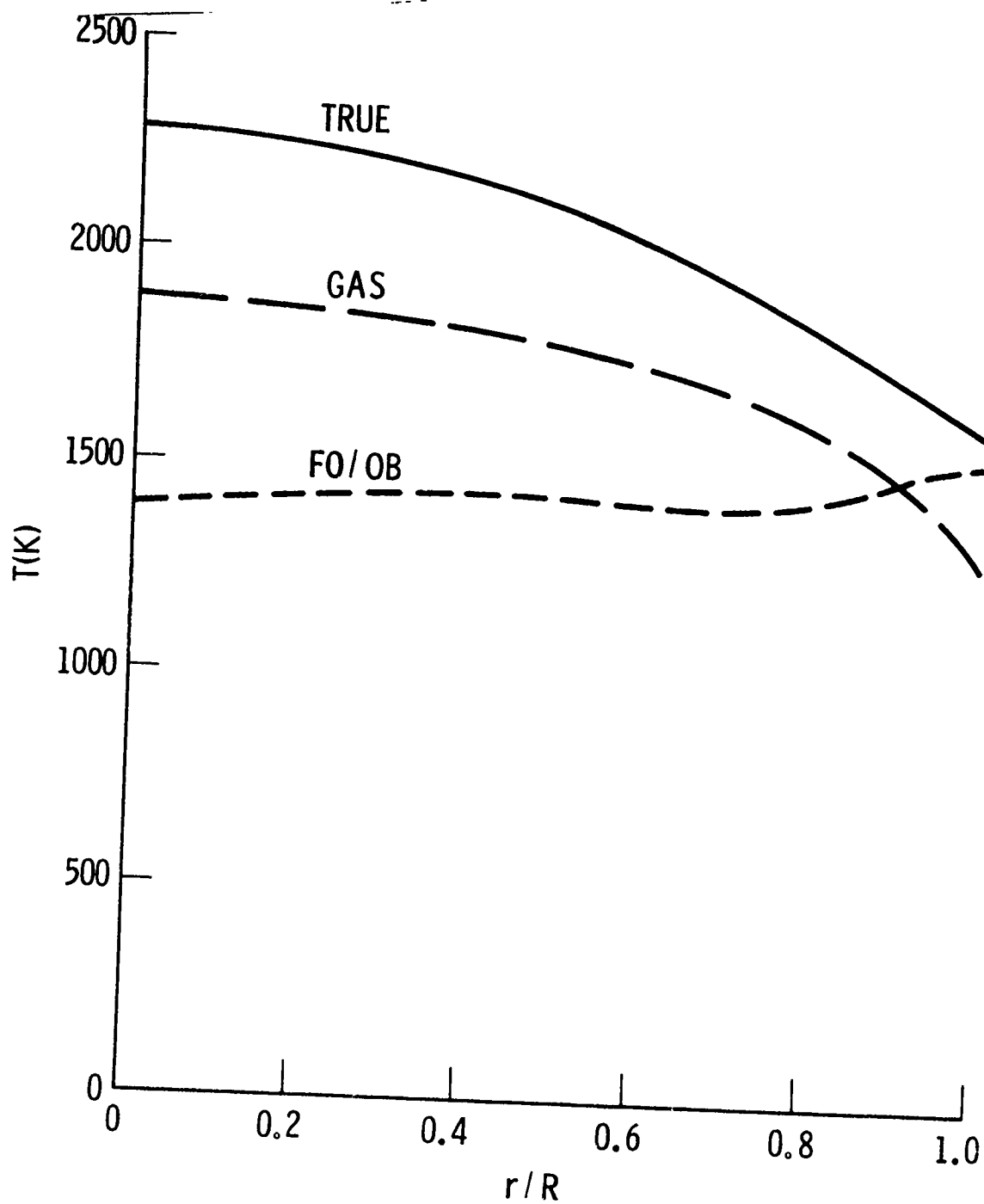


Fig. 26. Gas Temperature Retrieval Results for the ALP Plume Model

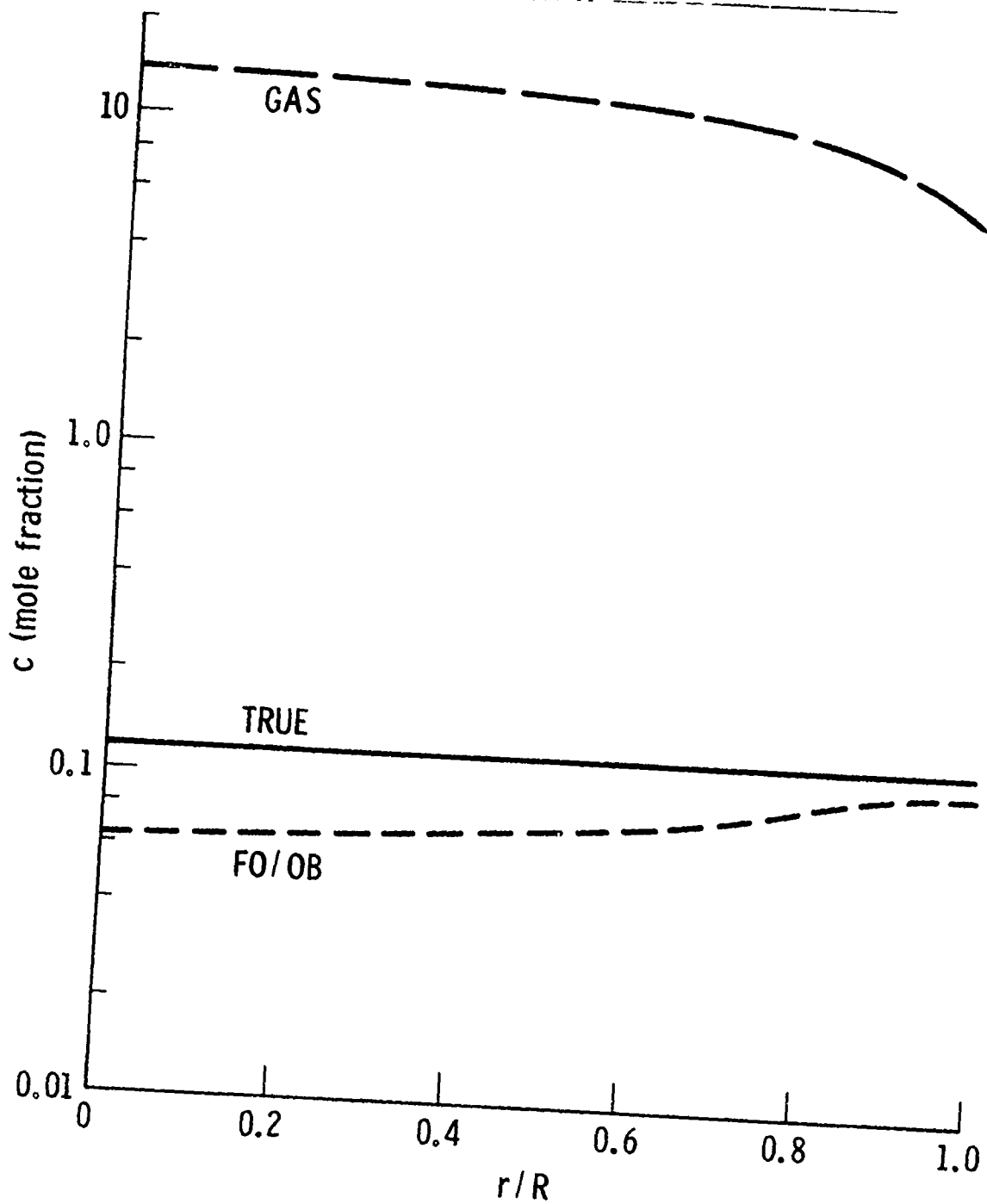


Fig. 27. Gas Concentration Retrieval Results for the ALP Plume Model

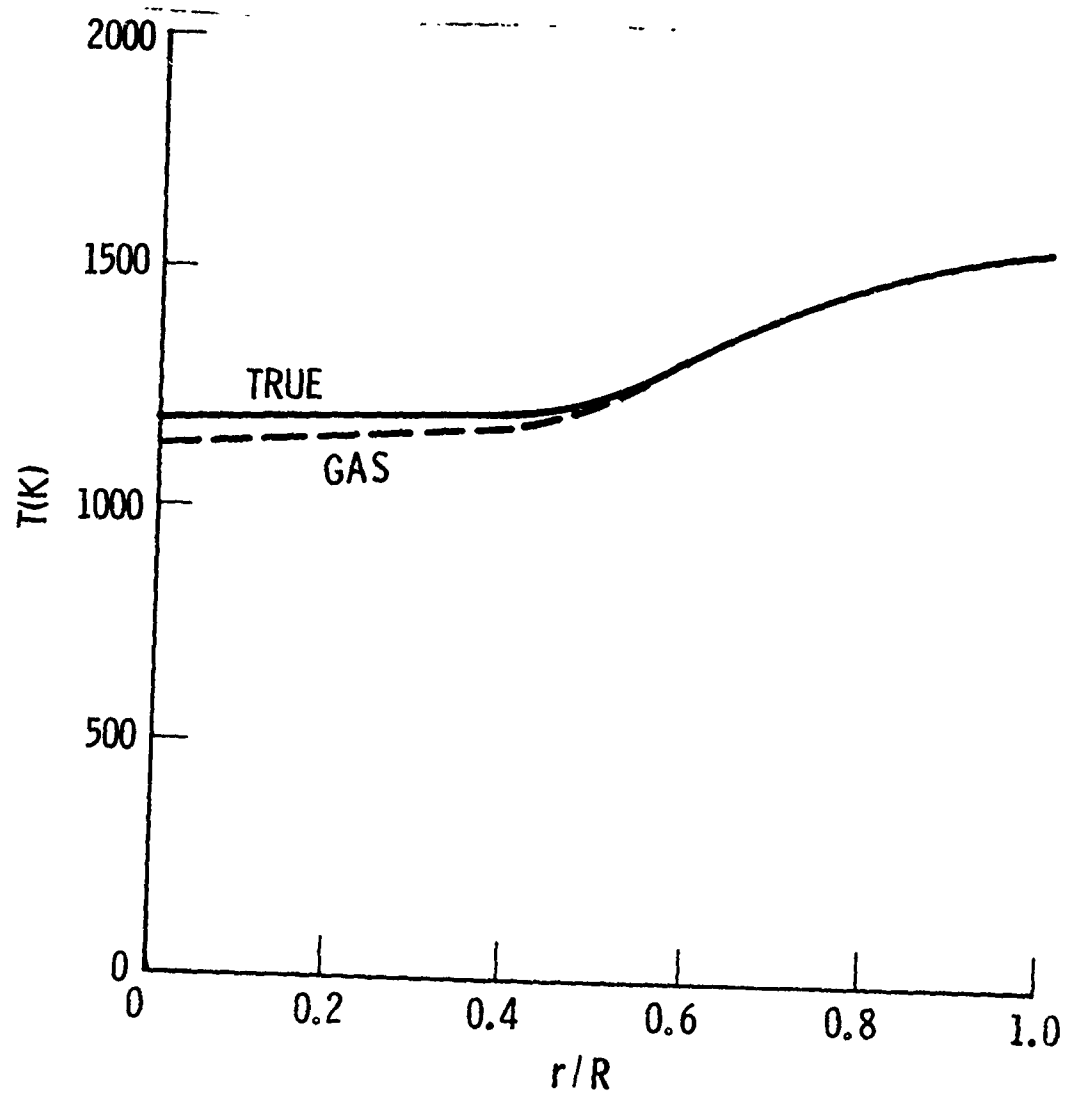


Fig. 28. Gas Temperature Retrieval Results for the RSP Plume Model

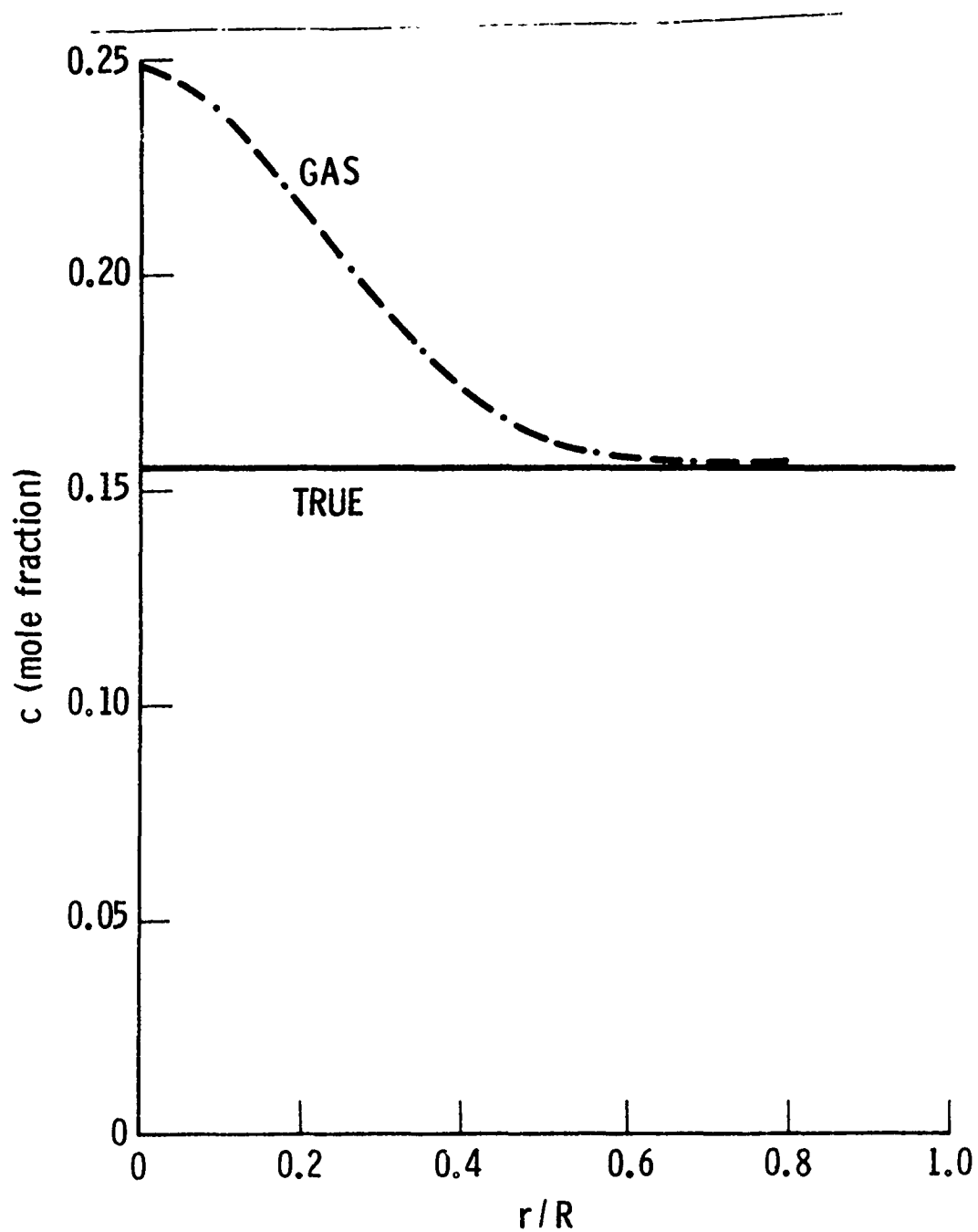


Fig. 29. Gas Concentration Retrieval Results for the RSP Plume Model

5. SUMMARY AND CONCLUSIONS

In the first phase of this work (Ref. 6), and repeated here, it was shown that even for plumes as lightly loaded with particles as the MSP and RSP models, the effects of particles could not simply be ignored in attempting to retrieve gas temperature and concentration from two-phase plumes. Retrieved temperatures were invariably too low, and concentrations were too high. With partial account of particle effects through the use of the first-order, off-band correction procedure, retrieval for these two lightly loaded plumes was substantially improved. For all practical purposes, the first-order correction procedure suffices as an accurate diagnostic for the gas properties of these plumes. For the more heavily loaded ALP plume model, however, even this correction procedure could not yield good gas retrieval results. In response to this problem, the fully-coupled gas-plus-particle retrieval procedure described in this report was developed. This new procedure is capable of arbitrarily accurate gas property retrieval from ideal data.*

In addition to the improved gas property retrieval procedure, a methodology for retrieving particle properties from appropriate E/A and laser scattering data was developed. These procedures were also shown able to retrieve particle properties to arbitrary accuracy from ideal data.

In all, the results of this work demonstrate that a complete diagnostics procedure for retrieving both particle and gas properties from two-phase, low-visibility propellant plumes could be developed. The fundamentals of the procedure have been developed and tested here. Additional work must be made

* A minor penalty of substantially increased computer running time is paid by using the fully coupled retrieval procedure over either the gas-only or first-order, off-band procedures.

on error propagation effects, and procedures for retrieving particle size and spatial distributions would enhance the value of the diagnostic.